

# Tagnoo: Enabling Room-Scale Smart Environments with RFID-Augmented Plywood

Yuning Su  
Simon Fraser University  
Burnaby, BC, Canada  
yuning\_su@sfu.ca

Yonghao Shi  
Simon Fraser University  
Burnaby, BC, Canada  
yonghao\_shi@sfu.ca

Tingyu Zhang  
Simon Fraser University  
Burnaby, BC, Canada  
tza80@sfu.ca

Xing-Dong Yang  
Simon Fraser University  
Burnaby, BC, Canada  
xingdong\_yang@sfu.ca

Jiuen Feng\*  
Simon Fraser University  
Burnaby, BC, Canada  
jiuenfeng@mail.ustc.edu.cn

Te-Yen Wu  
Florida State University  
Tallahassee, FL, United States  
tw23l@fsu.edu



Figure 1: (a) Tagnoo is a computational plywood, consisting of a plywood panel augmented with a grid of RFID tags. (b) Tagnoo can be used to construct office furniture like a table and chair, which are capable of sensing the presence of an object or user. (c) The heatmap image of the RSSI values captured while a user is seated at a desk using a laptop. The upper segment shows the sensor data obtained from the desk, while the lower segment shows the sensor data obtained from the chair.

## Abstract

Tagnoo is a computational plywood augmented with RFID tags, aimed at empowering woodworkers to effortlessly create room-scale smart environments. Unlike existing solutions, Tagnoo does not necessitate technical expertise or disrupt established woodworking routines. This battery-free and cost-effective solution seamlessly integrates computation capabilities into plywood, while preserving its original appearance and functionality. In this paper, we explore various parameters that can influence Tagnoo’s sensing performance and woodworking compatibility through a series of experiments. Additionally, we demonstrate the construction of a small office environment, comprising a desk, chair, shelf, and

floor, all crafted by an experienced woodworker using conventional tools such as a table saw and screws while adhering to established construction workflows. Our evaluation confirms that the smart environment can accurately recognize 18 daily objects and user activities, such as a user sitting on the floor or a glass lunchbox placed on the desk, with over 90% accuracy.

## CCS Concepts

• **Human-centered computing** → *Interaction devices*.

## Keywords

smart environment, computational material, RFID

## ACM Reference Format:

Yuning Su, Tingyu Zhang, Jiuen Feng, Yonghao Shi, Xing-Dong Yang, and Te-Yen Wu. 2024. Tagnoo: Enabling Room-Scale Smart Environments with RFID-Augmented Plywood. In *Proceedings of the CHI Conference on Human Factors in Computing Systems (CHI '24)*, May 11–16, 2024, Honolulu, HI, USA. ACM, New York, NY, USA, 18 pages. <https://doi.org/10.1145/3613904.3642356>

## 1 INTRODUCTION

The rapid advancement in computing technologies has led to a transformative vision, which aims to integrate computation into everyday materials, such as wood and textile, commonly used to

\*Jiuen Feng is also with University of Science and Technology of China.

Permission to make digital or hard copies of all or part of this work for personal or classroom use is granted without fee provided that copies are not made or distributed for profit or commercial advantage and that copies bear this notice and the full citation on the first page. Copyrights for components of this work owned by others than the author(s) must be honored. Abstracting with credit is permitted. To copy otherwise, or republish, to post on servers or to redistribute to lists, requires prior specific permission and/or a fee. Request permissions from [permissions@acm.org](mailto:permissions@acm.org).

CHI '24, May 11–16, 2024, Honolulu, HI, USA

© 2024 Copyright held by the owner/author(s). Publication rights licensed to ACM.

ACM ISBN 979-8-4007-0330-0/24/05...\$15.00

<https://doi.org/10.1145/3613904.3642356>

construct the physical environment [29]. This vision seeks to seamlessly combine sensing, computing, and wireless connectivity into these materials, thus enabling the creation of smart environments on an unprecedented scale. By imbuing computational and sensing capabilities into the very fabric of our surroundings, physical environments can actively sense and respond to users' daily activities, opening up a wide range of data-driven applications that can facilitate various life and work goals. Importantly, this can be achieved while maintaining the original appearance and functionality of the environment.

Despite the promising prospects, realizing this vision is accompanied by substantial challenges. From a sensing perspective, a significant obstacle lies in the limited capability of existing computational materials to function without wire connections for power, computation, or data communication. Prior research on wood or textile sensors has revealed that the majority of them rely on wire connections to external devices and batteries [96–98, 107]. Another critical challenge is the materials' inability to maintain functionality in the presence of damage during the fabrication process, such as cutting and screwing. Despite some prior works equipping materials with basic computing and wireless connectivity, their sensors fail to survive common fabrication operations, such as cutting [34, 35]. Consequently, the majority of existing work cannot function as a material and cannot be seamlessly integrated into the established workflows and tools used by workers to construct physical environments.

This paper introduces Tagnoo, a computational plywood prototype that addresses the aforementioned challenges associated with the development of room-scale smart environments using computational materials. Tagnoo is a plywood panel augmented with a grid of Radio Frequency Identification (RFID) tags (Figure 1a). Tagnoo can be used to construct office furniture such as tables, chairs, and shelves as well as building infrastructure like floors to detect the presence of everyday objects and users - such as a person typing on a laptop at a table (Figure 1b and c). Tagnoo stands out as a battery-free and cost-effective smart plywood prototype capable of withstanding common woodworking operations, such as sawing, nailing, or screwing. It allows woodworkers to seamlessly incorporate it into their projects without requiring specialized technical or engineering skills. Additionally, Tagnoo maintains a form factor that is nearly identical to regular plywood, eliminating the need for electrical connections to external devices like microcontrollers or wireless communication modules.

An important aspect of Tagnoo is its compatibility with woodworking techniques, allowing for the creation of household items using plywood without disrupting established workflow. Although some RFID tags may be susceptible to damage during woodworking operations, the majority of them remain intact and fully functional in the final product. Once the items, such as desks and shelves, constructed with Tagnoo are completed, RFID readers can retrieve the signals from the tags. The presence of RF-absorbing objects placed on the sensor surface, such as a glass lunchbox or a laptop on the desktop, may hinder the propagation of RF signals and subsequently impact the signal strength of the tags (Figure 1c). By carefully analyzing the readings obtained from each individual tag, our system can recognize diverse objects using machine learning

techniques. This data can subsequently be used to infer user activities, enabling new applications for contextual interactions or personal reflection.

The design and implementation of our prototype were informed by a series of experiments aimed at examining the various parameters that may impact the sensing performance. These parameters included the type of RFID tags used, the arrangement of the tags, the optimal depth at which the tags should be placed inside the plywood, and the adhesive strategy used to affix a veneer layer on top of the tags. Additionally, we evaluated the potential effects of some of the common woodworking operations, such as cutting, screwing, and painting, on each individual tag as well as the overall sensing performance of the remaining plywood sensor. To validate the effectiveness of our approach, we invited two experienced woodworkers to construct a small office environment using the Tagnoo. This environment consisted of a desk, chair, shelf, and floor, all crafted using conventional tools such as a table saw and screws while adhering to established construction workflows. Subsequently, we conducted tests to assess the recognition accuracy of the smart environment for 18 daily objects and simple user activities, such as a user sitting on the floor or a glass lunchbox placed on the desk. Our findings revealed that our system achieved an accuracy rate of over 90%.

Our research centers on advancing computational materials and their integration into practical use. In this context, it makes three key contributions. Firstly, it demonstrates the creation of a room-scale smart environment using well-established tools and workflow commonly employed by woodworkers, without the need for a technical background. Secondly, it presents experimental results that investigate the factors influencing sensing performance and the potential impact of woodworking operations such as cutting, screwing, and painting. Lastly, it evaluates the sensing accuracy of some of the common daily objects and simple user activities within the smart environment.

## 2 RELATED WORK

In this section, we provide a concise overview of the background and existing literature in the area of computational materials, RFID sensing, and sensor deployment for smart environments.

### 2.1 Computational Materials

"Computational materials" is a term coined by Gregory Abowd, which refers to everyday materials that possess embedded computational capabilities or wireless sensors that seamlessly integrate into the material itself [29]. The concept of computational materials can be traced back to 1998 with the introduction of the Musical Jacket [73]. This innovative garment featured a fabric-based touch keypad, enabling users to interact with a computer using the jacket itself. Since then, extensive research efforts have been devoted to the advancement of interactive materials [48, 72, 75, 76, 96, 97]. A notable example relevant to this research is Capacitivo, developed by Wu, et al. [97]. Capacitivo features a fabric sensor that uses capacitive sensing to recognize the objects in contact with it. This broadens the range of applications for interactive materials, allowing for more intuitive and seamless user interactions.

Recent advancements in materials science and manufacturing have greatly accelerated progress in computational materials. These materials can now be produced at a low cost [35, 37, 98, 103], and



even operate without the need for a battery [33, 34, 103], bringing practical applications within reach. For instance, the development of triboelectric nanogenerator (TEENG) technology demonstrates the ability to convert mechanical energy to electrical energy [94, 95]. This breakthrough has paved the way for creating batteryless computational materials [33, 34]. One example of this progress is SATURN and MARS [34, 35], where researchers have successfully designed a batteryless paper microphone. This novel device utilizes TEENG to sense audio sounds from users and employs backscatter to eliminate the need for a battery. Another development in this field is the integration of TEENG into plywood, known as iWood [98]. By optimizing the structure of TEENG, researchers have ensured that the sensor remains functional even during common woodworking operations. This integration enables the fabrication of everyday objects that are inherently embedded with vibration sensors, expanding the possibilities for incorporating computational capabilities into various household items.

Despite the significant progress made in the field of computational materials, most existing materials lack the capability to operate without wire connections for power, computation, or data communication. Moreover, most of them are incapable of sustaining their functionality in the event of damage during the fabrication process, such as cutting and screwing. In light of existing research, our work introduces a new method, which aims to create computational materials that effectively address these limitations. The proposed approach involves the integration of RFID tags into plywood, thereby imbuing the material with limited sensing, computing, and wireless connectivity capabilities, while still retaining the inherent characteristics of traditional plywood.

## 2.2 RF Sensing

Radio frequency (RF) signals have a rich history of utilization in the detection and tracking of objects, humans, and environmental changes [43, 86]. The underlying principle involves the transmission of a radio signal, followed by the observation of the reflected signal. This reflected signal contains information about the material composition, shape, size, orientation, and even movement patterns of nearby objects. By analyzing these reflected signals, a system can facilitate a wide range of applications, including the recognition of human activities [39, 62, 64, 68, 83, 85, 93, 107], the identification of gestures [32, 85, 92, 96], the monitoring of vital signs [30, 49, 82], the localization of indoor positions [66, 109], the identification of individuals [47, 56], and the recognition of objects [44, 60, 63, 80, 88, 104]. These advancements highlight the potential of RF sensing technology. Moreover, RF sensing offers distinctive advantages over alternative sensing approaches, as it can effectively identify objects that are obstructed by barriers and can even discern the materials comprising those objects. Building upon this foundation, our work aims to incorporate RF sensing into computational plywood, thereby enabling object recognition capabilities.

The RF-based technique that is directly relevant to our research is RFID. RFID is a specialized RF technology primarily used for the purpose of identifying and tracking objects or people using RFID tags. These tags are composed of a small chip and an antenna that can store and transmit data wirelessly to RFID readers. When an RFID reader emits an RF signal, it powers the tag, prompting it to respond

with the information it holds. The applications of RFID technology are vast, with significant usage in supply chain management [89], asset tracking [46, 74], inventory control [81, 110], access control systems [78], and contactless payment methods [31]. Its versatility lies in its ability to operate at different radio frequencies, with the high-frequency range (13.56 MHz) and ultra-high frequency range (915 MHz) being the most popular for RFID systems. In HCI, both HF and UHF RFID have been utilized to track the location and orientation of objects [67, 87]. UHF RFID has demonstrated significant potential in various applications owing to its shorter wavelength, higher reading rates, and extended sensing range. Beyond object identification, UHF RFID tags possess the capability to enable functionalities such as activity recognition [30, 53, 69, 84], touch sensing [55, 77], shape awareness [58, 90], material identification [51, 91, 101, 108], person identification [47], and object imaging [91]. However, a significant challenge in deploying UHF RFID tags lies in the integration process, which demands substantial time, effort, and technical expertise from workers. Overcoming this obstacle is crucial to harness the full potential of UHF RFID technology. In response, our work demonstrates an approach that involves the integration of dense arrays of RFID tags into materials, specifically plywood. This approach empowers woodworkers to effortlessly and implicitly deploy an extensive network of RF tags across different items within an environment. By embedding RFID tags into plywood, the deployment process becomes simplified, enabling efficient and widespread adoption of UHF RFID technology in various contexts.

## 2.3 Sensor Deployment for Smart Environments

Smart environments are physical spaces that incorporate a range of computing and interface devices, working in tandem to enhance the overall quality of life, optimize resource utilization, and deliver personalized services to the individuals residing within these environments [41, 71]. Several key components are required to establish such smart environments, including connected sensors [59, 79], actuators [79], data processors [42], AI technologies [102], and software platforms [54]. However, deploying connected sensors is considered the foundational step among these components, as they play a critical role in collecting and providing data to the system, thereby driving its intelligence.

One widely adopted approach for deploying connected sensors in various environments involves directly attaching sensing devices to existing infrastructure in an ad-hoc manner [50, 52, 57, 62, 105, 106]. Extensive prior research has employed this approach by installing electromagnetic (EM) [40, 50, 62, 83, 107], vibration [52, 57, 99, 106], and light sensors [61, 65, 103] within the environment to detect and monitor user interaction and activities. For example, *ElectriSense* [50] installs sensors on power outlets, utilizing electromagnetic interference in powerlines to identify appliances. Similarly, *Wall++* [107] utilizes painted antennas and sensors on walls to capture airborne EMI signals, enabling the detection and localization of appliances. Another notable work, *StarLight* [65], deploys sparse photodiodes on the floor to receive light signals and reconstruct human posture. Furthermore, efforts have been made to install vibration sensors or tags on floors and walls [106], as well as plumbing, gas, and HVAC infrastructure [105] to detect user activities.

However, it is worth noting that the integration of sensors into existing spaces through current ad-hoc methods often results in devices that are visually conspicuous and do not seamlessly blend with the surroundings. While this lack of integration can be mitigated by concealing the sensors more effectively within the environment [107], this process typically requires expertise in electronics and engineering, thereby posing challenges for workers without a technical background.

In summary, our research stands out from the existing literature for its unique focus on the advancement of computational materials and their integration into practical use. Tagnoo is developed to withstand operations such as cutting, nailing, and screwing. This sets our work apart from many existing approaches as their sensors did not involve the same use of materials, causing them to break upon encountering such operations. Furthermore, unlike many other existing works, our approach does not rely on wired connections for power, computation, and data communication. This ensures that Tagnoo can seamlessly integrate into existing woodworking workflows and tools without requiring workers to acquire new skills unrelated to their domain, such as electronics or engineering.

### 3 DAYS IN THE LIFE OF A TAGNOO USER

Tagnoo is a computational plywood that functions just like traditional plywood materials, suitable for a variety of applications in both residential and commercial settings. Its main goal is to facilitate the development of smart environments when Tagnoo serves as an alternative of plywood materials for woodworkers and consumers in their projects. For example, woodworkers can choose Tagnoo for constructing furniture or as a flooring material during home construction and renovation projects. As such, Tagnoo's direct target audience is primarily woodworkers and users who engage in furniture assembly. However, from the perspective of end-users, residing within a Tagnoo environment offers advantages through seamless and implicit interaction with the computer system. This interaction enables the deployment of various data-driven applications, which in turn assist users in achieving their personal and professional goals. This section provides an illustrative example of typical days for a Tagnoo end user.

Alice, a first-year college student, is preparing to move into her new rental place before the start of her first semester. Prior to her move, she decides to renovate her room with new furniture and flooring. Her desired furnishings include a desk, chair, bookshelf, and other necessary items like a bed frame. Due to a limited budget and tendency to having personalized items, Alice chooses the DIY route for her furnishings. She visits a hardware store to purchase conventional plywood, Tagnoo materials, Tagnoo-enabled floor planks, and other necessary building components and tools. With the assistance of her brother, who is a skilled carpenter, she installed the floor planks in her room (Figure 2a). Once the floor installation was complete, they proceeded to cut both the traditional plywood and Tagnoo into smaller segments to create the furniture pieces (Figure 2b). Familiar with furniture assembly from past projects, they assemble the furniture using screws (Figure 2c). It should be noted that Alice recognizes that some of the sensing functionalities provided by Tagnoo could potentially be achieved through alternative technologies, such as using a smartwatch or installing ad-hoc sensors on the furniture. However, she opted for Tagnoo as

it instantly transforms her environment into a smart living space without requiring any additional technical aspects on installing them.

After moving in, Alice can configure her desk to log her daily activities and work progress, allowing it to respond accordingly. For instance, the desk and chair can detect and record events such as the duration of laptop usage or periods of non-usage. This can be inferred by the presence or absence of her laptop on the desk or in her bag placed on the chair during holidays (Figure 2d). The information collected can be used to provide Alice with insights into her work practices, facilitating personal reflection and potentially even offering insights into her psychological state during work. In addition, the bookshelf can detect and log Alice's reading habits by tracking when she takes her book from the shelf and returns them (Figure 2e). If this routine is disrupted, especially during a busy week before a school project deadline, the change in behavior can be logged for Alice to review at a later time. Furthermore, the desk can also detect the placement of objects such as chocolate bar or a glass lunch box, with or without her favorite rice dish. This information can be used to infer details about Alice's diet. When combined with the duration of her preferred floor-sitting exercise routine sensed by the floor, the system can provide her with insights into her health, well-being, and lifestyle choices.

## 4 TAGNOO DESIGN AND IMPLEMENTATION

Tagnoo consists of a grid of RFID tags embedded within a plywood panel to sense objects and users in the environment. Each RFID tag functions as a "pixel" within the panel, enabling the system to perceive changes in the environment by detecting blockages or alterations in the strength of RF signals caused by the presence of different objects and humans. Our development of Tagnoo began with an investigation on the integration of RFID tags into the plywood substrate in a reliable manner while ensuring their sensitivity not significantly degrading. This involved a series of preliminary experiments, aimed at exploring suitable RFID tag types, tag densities, depths for embedding the tags, and various adhesive strategies used to affix a veneer layer on top of the tags. Throughout these experiments, a UHF RFID Reader from Impinj Speedway (Revolution R420) and UHF RFID Antenna (Vulcan 262006) were used to measure the signal strength of the RFID tags

### 4.1 Experiment 1: Tag Types

UHF RFID tags are available in various sizes and shapes, each tailored to meet specific application requirements. Our study focused on identifying a UHF RFID tag that could be seamlessly integrated into plywood, effectively operate in a dense configuration, and maintain a consistent reading regardless of its orientation. Since RFID tags may be positioned in various orientations inside furniture or floors, we needed to select a tag to accommodate these variations.

*Tag pre-selection.* Our selection process was guided by four criteria. First, the RFID tags should be easily cut or drilled to prevent obstruction during woodworking operations. Secondly, they need to be relatively small to allow for a decent sensing resolution in a 2D space when arranged in a grid layout. Thirdly, the reading range of the RFID tags should be sufficient to cover the size of

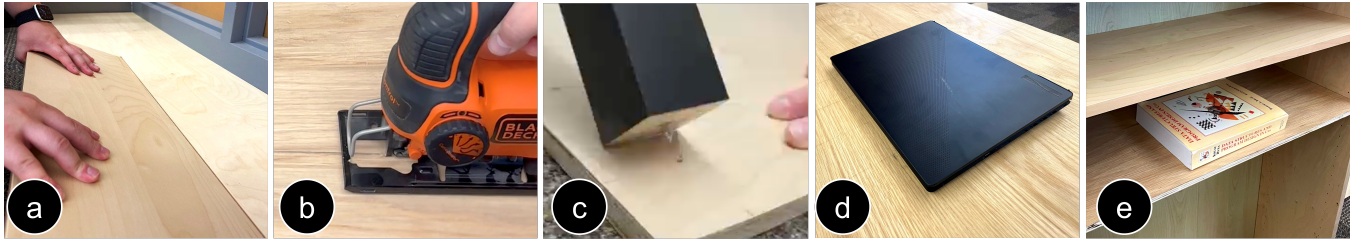


**Figure 2: An illustration of use scenarios of Tagnoo.** Tagnoo can be easily (a) installed as floors, providing seamless integration into the physical environment. Additionally, it can be (b) cut into small pieces and (c) assembled into furniture. The physical environment created using Tagnoo can sense user activities and daily routines by detecting various events through the presence of personal items and objects. For instance, (d) a laptop left on the table for an extended period could indicate that the user is away from work, possibly on vacation. (e) If a user’s favorite book remains on the bookshelf during the user’s designated reading time for several days, it could signify a change in the user’s routine.

a room. Lastly, the RFID tags should be reliably detected regardless of their orientation to the RFID antenna. We investigated 24 widely available RFID tags, including those with and without enclosures, and with varying sizes and reading ranges [1–24]. We cut and drilled the tags with enclosures and compared their resistance to that of regular plywood, concluding that enclosures hinder woodworking operations. Consequently, tags with protective shells [1, 10, 12, 15, 22] were excluded. Additionally, tags with footprints exceeding 10 cm on any side were disregarded [6, 9, 17–21], as they would be too large to be arranged in a dense grid for accurate sensing. Further, tags with a reading range shorter than 5 meters were not considered [3–5, 11, 16], as they may not be reliably detected at a room-scale. The remaining tags were either circularly polarized or linearly polarized.

**Orientation effect.** To evaluate the reliability of the remaining tags at different orientations to the RFID antenna, we conducted an experiment using two specific tags: Impinj H47 [13] and Impinj E62 [25]. The Impinj H47 was chosen due to its widespread use as a circularly polarized tag. Additionally, the Impinj E62 was selected to assess the performance of a linearly polarized tag, given its similar size to the Impinj H47 tag. While these tags may not represent the most optimal options in terms of size or sensitivity, they were suitable for gaining insight into the performance differential between circularly and linearly polarized tags.

In our experimental setup, we carefully arranged each type of RFID tag under investigation into a  $3 \times 3$  array configuration. The distance between the centers of adjacent tags was precisely set at 10 cm from one another. The purpose of our measurements was to evaluate the sensitivity of the tags in four different orientations:  $0^\circ$ ,  $30^\circ$ ,  $60^\circ$ , and  $90^\circ$ . For the circularly polarized tags, we excluded the  $90^\circ$  angle from testing to avoid duplicating results, as it is identical to the  $0^\circ$  angle. To ensure consistency, each reading phase was conducted for a duration of 3 minutes (approximately 6000 sample points per tag). Throughout the experiments, all the tags were positioned below the RFID antenna, and they were placed on top of a plywood surface. We retrieved RSSI from the RFID reader to measure the sensitivity of tags. To minimize the potential influence of tag location with respect to the RFID antenna, we calculated the average RSSI based on the data from all the tested tags.

**Result.** Figure 3 illustrates the results of the experiment. All of the circularly polarized tags demonstrated consistent readability, maintaining a stable RSSI across the four tested orientations. In contrast, the orientation of linearly polarized tags significantly impacted their RSSI. Specifically, during the 3-minute reading periods at  $0^\circ$  and  $30^\circ$  conditions, two and seven tags, respectively, could not be detected. Thus, we opted to incorporate circularly polarized tags into our prototype. Note that the close proximity between linearly polarized tags might affect their sensitivity, causing their RSSI to be lower than that of circularly polarized tags. Nevertheless, this fact does not alter our decision, because our decision was made based on the rationale that furniture in a smart environment should not be restricted to a specific orientation and should remain interactive even when rotated by the user.

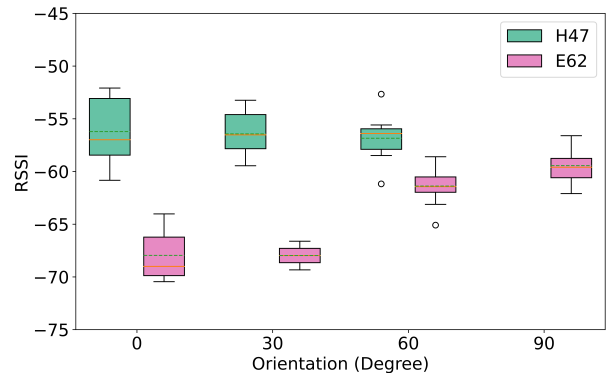


**Figure 3: RSSI of the E62 linearly polarized and H47 circularly polarized tags placed in different orientations.** (The solid orange line indicates the median, while the dashed green line represents the mean in all figures. The variations in box size and error bars demonstrate more noticeable signal differences from RFID tags at different positions within the  $3 \times 3$  grid (also shown in Figure 6, Figure 7, Figure 8 and Figure 10). However, these variances are smaller when tag locations remain the same (as shown in Figure 4, Figure 5, and Figure 9).

## 4.2 Experiment 2: Tag Grid Density

This study aimed to examine the impact of the density of circularly polarized tag grids on tag readings. It is generally observed that a denser arrangement of tags results in a higher 2D sensing resolution, which is particularly advantageous for capturing subtle human activities and small objects in the environment. Furthermore, a denser arrangement is less susceptible to the loss of the sensing region within the plywood sensor caused by damage to the tags during woodworking operations like sawing, nailing, or screwing. However, the potential drawback of a denser tag arrangement is the possibility of interference between adjacent tags, leading to a decline in RSSI. Hence, our experiment aimed to determine the maximum density of RFID tags that can be used in our implementation without compromising RSSI. Like our previous experiment, we positioned the circularly polarized RFID tags in a  $3 \times 3$  grid below the RFID antenna. The distance between the centers of adjacent tags was varied, ranging from 6 cm to 15 cm. To investigate the interference of the surrounding tags on the central tag, we calculated its RSSI. To avoid tag overlap at close ranges, distances below 5 cm were excluded from this experiment.

*Result.* The results of this experiment are illustrated in Figure 4. Our findings indicate that the distance between tags has an effect on the RSSI. Specifically, we observed an improvement in RSSI as the distance between the centers of adjacent tags increased from 6 cm to 10 cm. However, once the distance exceeded 10 cm, we noticed a stabilization of RSSI, suggesting that the influence of adjacent tags on signal strength becomes minimal. This finding has implications for the design and deployment of our tag-based system. It suggests that maintaining a minimum distance of 10 cm between tags can optimize signal strength and minimize interference. Beyond this distance, the impact of adjacent tags on RSSI becomes negligible. However, it is important to note that there are trade-offs associated with increasing the distance between tags. One such trade-off is the effect on sensing resolution in a 2D space. If the target applications require a higher tag resolution, such as sensing a cup with a diameter of less than 10 cm, a balance needs to be struck. In such cases, it may be necessary to compromise on the optimal signal strength to ensure accurate object detection.

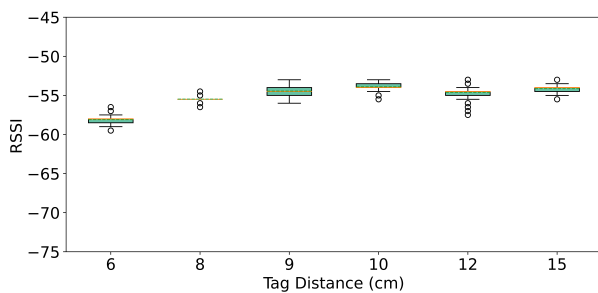


**Figure 4: RSSI of the RFID tags placed at different distances from each other. The small variances in box size and error bars are due to the use of a single RFID tag to obtain the RSSI values in each condition (same in Figure 5 and Figure 9).**

In certain scenarios, particularly those involving activities on the floor, the close arrangement of RFID tags may not always be

necessary. Objects of larger size, such as feet in these scenarios, obstruct the propagation of RF signals over a wider area, allowing for a sparser arrangement of tags while still effectively detecting them. This approach offers the potential for reduced manufacturing costs. Thus, we conducted an additional experiment to investigate the minimum density at which tags can be arranged without significantly compromising the resolution of 2D sensing. The specific focus of our experiment was to determine the maximum horizontal distance at which a tag can detect an object (fist in our case), which measured approximately 10 cm in length. To carry out the experiment, a single tag was positioned beneath the RFID antenna, and the distance between the object and the tag was systematically varied from 10 cm to 30 cm, with an increment of 5 cm.

*Result.* The results of this experiment are illustrated in Figure 5. When the object is positioned within a distance of 15 cm from the RFID tag, there is a notable decrease about 7 dB in RSSI compared to the scenario without an object. This substantial change suggests that the presence of the object within this close proximity significantly affects the tag's reception of RF signals. However, beyond a distance of 20 cm, this effect gradually diminishes and eventually becomes indistinguishable from the situation where no object is present.

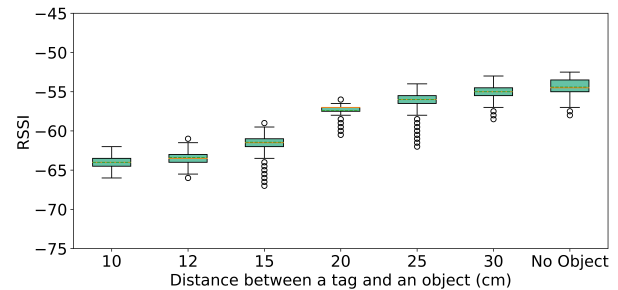


**Figure 5: RSSI of an RFID tag at varying distances from a fist.**

Based on the results obtained from our experiment, we determined the maximum and minimum distances between adjacent tags. These findings hold implications for the development of Tagnoo in various item categories. For furniture items, such as desks, which commonly come into close contact with relatively smaller objects like lunchboxes, it is advisable to utilize a Tagnoo system with a dense tag arrangement. After careful consideration of available options, we have chosen a 10 cm distance in our implementation of plywood material with a high tag density. This decision was made to maximize signal strength, considering the marginal increase in 2D resolution compared to a relatively large loss in signal strength (e.g., approximately 2 dB drop from 10 cm to 8 cm). On the other hand, when it comes to larger infrastructure components like floors, which typically encounter objects with larger footprints, such as feet, a more cost-effective approach can be adopted. In our implementation, we have positioned the Tagnoo tags at a distance of approximately 30 cm for plywood material with a low tag density (maximum 15 cm away from an object). This has led to a reduction in the fabrication cost of the system. Furthermore, we have adopted a 20 cm distance for the plywood materials with medium tag density.



### 4.3 Experiment 3: Depth of Embedded Tags

Plywood is a composite material that is formed by bonding multiple layers of wood veneers together. The face side of plywood typically shows a smoother and visually appealing surface. In our implementation, we have strategically embedded RFID tags within the veneer layers near the face side. It is thus important to consider the potential impact of the thickness of the top veneer layer on the signals emitted by the RFID tags. To investigate this, we conducted an experiment by embedding the  $3 \times 3$  RFID tags within the veneer layers at varying depths from the plywood's face surface. We examined the changes in signal strength across different thickness levels, including a 0.025 cm (0.01 inches) veneer and plywood sheets ranging from 0.32 cm to 2.54 cm thick.

*Result.* The results of this experiment are illustrated in Figure 6. It can be observed that the RSSI decreases as the thickness of the plywood layers increases. Specifically, when a veneer layer measuring 0.025 cm thick is placed over the RFID tag, there is a reduction of 1.7dB in the RSSI. Furthermore, as the thickness of the veneer layer increases beyond this point, the decrease in RSSI exceeds 3dB. For our implementation, we opted to cover the RFID tags with a veneer layer that is 0.025 cm thick to maximize signal strength.

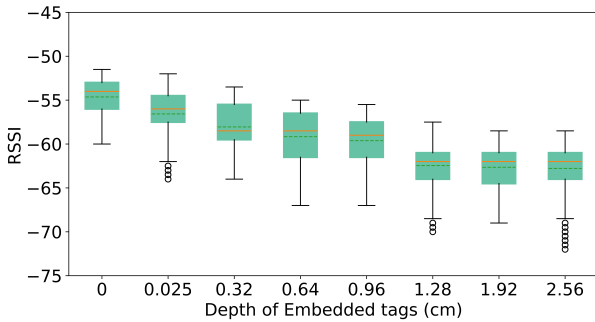


Figure 6: RSSI of the RFID tags placed at varying depths from the plywood's face surface.

### 4.4 Experiment 4: Gluing Strategies

During the fabrication process, a layer of veneer needs to be adhered to the RFID tags and plywood substrate. However, the sensitivity of these tags may potentially be compromised when covered with wood glue due to the moisture present in the glue. To understand the effects of wood glue on RFID tag performance, we conducted an experiment to evaluate its impact on the signal strength. Since the RFID tags are positioned near the face surface of the plywood, our investigation focused solely on examining the effects of wood glue applied on top of the  $3 \times 3$  tags. Three adhesive strategies were tested: (1) Full Coverage, where both the RFID tags and the gaps between them were completely covered with glue, resulting in a uniform distribution of glue across the entire surface of the plywood panel's interior (Figure 7a). (2) Gap Filling, which involved filling only the gaps between the RFID tags and the edge of the plywood with glue, ensuring that the top surface of the tags remained glue-free (Figure 7b). (3) Edge Application, where the glue was exclusively

applied to the four edges of the plywood panel's interior. This approach allowed the top surface of the tags and the majority of the surrounding gaps to remain free of glue (Figure 7c). To cover the tags, a veneer layer with a thickness of 0.025 cm was used. For the purpose of this study, Gorilla Wood Glue was chosen due to its widespread usage in woodworking applications.

*Result.* The experimental results are depicted in Figure 7d. Our findings indicate that applying wood glue directly onto the surface of RFID tags significantly attenuates the RSSI. However, when the glue is used solely to fill the gaps between the tags and the edges of the plywood, its impact on RSSI is minimal. As illustrated in Figure 7d, there was a negligible difference in RSSI between Gap Filling and Edge Application. However, Gap Filling, due to its larger surface area for adhesion, potentially offers stronger bonding between the veneer and plywood substrate compared to Edge Application. Therefore, in our implementation, we apply wood glue exclusively to these gaps.

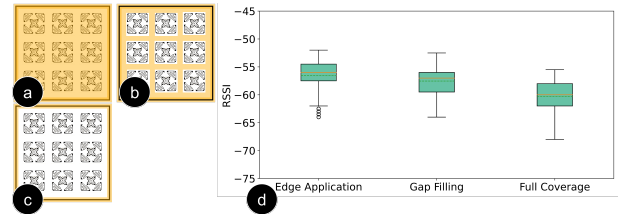


Figure 7: An illustration of different gluing strategies that were investigated in our study, which include (a) Full Coverage, (b) Gap Filling, and (c) Edge Application. The regions highlighted in orange indicate the areas that were covered by glue. (d) RSSI of the RFID tags shown by different gluing strategies.

## 5 UNDERSTAND THE IMPACT OF WOODWORKING OPERATIONS

Woodworking operations, such as sawing or painting, may potentially impact tag signals or cause damage to the tags. While it is possible for the system to rely on the remaining unaffected tags, the extent to which woodworking operations impact the functionality of the affected tags remains unclear. We conducted a series of experiments to address this question, specifically targeting common woodworking operations such as sawing, screwing, nailing, and painting.

### 5.1 Experiment 5: Sawing

The goal of this experiment was to investigate the potential consequences of using a saw to cut plywood and its impact on RFID signals. We aimed to examine the impact of a damaged antenna on the signal strength of RFID tags. Specifically, a completely broken chip definitely leads to tag malfunction, but since our RFID tag has four antennas located at the corners, it is uncertain whether a tag, with a single cut leaving only two antennas, would still maintain its functionality. To investigate this, we included two common scenarios where tags undergo a straight-line saw cut: partially cut and fully cut. The partially cut condition aimed to replicate cuts

that only damaged the antennas of the RFID tags (Figure 8a), while the fully cut condition was designed to assess the impact when both the antenna and the matching circuit are damaged (Figure 8b). We have intentionally excluded scenarios where the cut deviated from a straight line, as our discussion with woodworkers has indicated that the majority of common woodworking practices involve cutting panels in straight lines.

We conducted our experiment using a  $3 \times 3$  array of RFID tags placed on plywood, with a distance of 10 cm between each tag. To simulate antenna damage, we deliberately cut a half portion and full portion of two antennas on the tags, as illustrated in Figure 8. To determine whether the polarity of the tag changes when only two antennas remain, we also tested their signal strength under a 90-degree rotation.

*Result.* The results of this study are presented in Figure 8, which includes a tag without any damage as a baseline. Encouragingly, the tested tags demonstrated resilience even when their antennas were partially damaged, although there was a noticeable decrease in RSSI. We did not observe a significant change in the tag's polarity, as the RSSI values of the rotated tags were similar to those of tags without rotation. However, when the antennas were fully damaged, the tags ceased to function. We suspect that this is because the damage extended to the impedance matching circuit, located within 1.25 cm of the tag's center. It is important to acknowledge that these results may vary depending on the specific characteristics of each tag. Nonetheless, this study highlights that our current implementation can withstand sawing during woodwork to a certain extent. From a sensing perspective, the most unfavorable outcome would be the loss of 10cm wide sensing areas along the edges of a cut board, which appears to be acceptable. The primary objective of this study was to investigate the damages caused by a saw. However, it is reasonable to infer that the findings can be extrapolated to damages caused by drills. Although drills may have different action characteristics, they share common features with saws in terms of the resulting damage to the tag, particularly in causing an open cut. Therefore, it is plausible to generalize the observed patterns in this study to damages caused by drills.

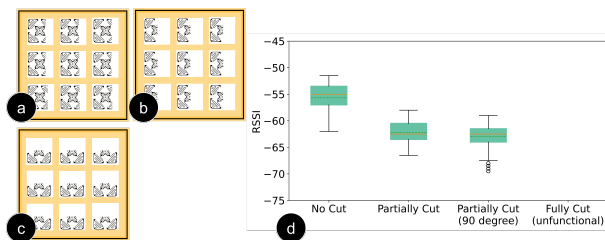


**Figure 8: An illustration of how RFID tags were cut in our experiment: (a) One side of the tag's antennas was partially cut; (b) One side of the tag's antennas was fully cut; (c) the condition shown in (b) rotated by 90 degrees counterclockwise; (d) RSSI of the RFID tags shown by the cutting conditions.**

## 5.2 Experiment 6: Screwing

When inserting screws or nails, there is a potential for damage to occur to a tag. However, the nature of this damage may differ from

that caused by cutting or drilling. This is due to the conductive property of screws, which allows for a capacitively coupled connection to the antenna. As a result, the screw may act as an extension of the antenna, enabling it to receive and emit RF signals. In order to understand the impact of screws on tag functionality, we conducted a study in which we inserted screws at various positions of an RFID tag affixed to a plywood surface. The purpose of this study was to investigate the effects of screw placement on tag performance. Figure 9a-c illustrates the three specific locations we selected for screw insertion: (1) on the outer antenna, (2) on the inner antenna, and (3) directly on the chip. These positions were chosen to cover some of the most common scenarios for potential damage to RFID tags.

*Result.* Figure 9d presents the collected RSSI data for the various tested positions, along with a baseline measurement taken without any damage. Our findings suggest that the tags were able to withstand being screwed in as long as the screw did not cause any damage to the chip. Interestingly, unlike cutting, screw damage occurring on the inner antenna, close to impedance match circuit, did not result in the tag ceasing to function. Instead, it only caused a slight decrease in the RSSI. This observation can be attributed to the conductive nature of the screw, which allows it to act as a functional component of the tag. It is worth noting that this damage-prone area only accounts for a mere 6% of the total tag area. Upon careful observation, no significant fluctuations in the RSSI values were detected.

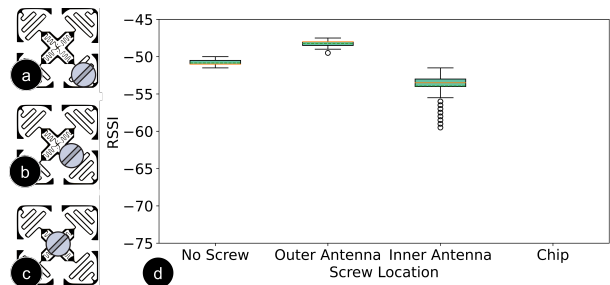


**Figure 9: An illustration of the three different locations where the screw was applied: (a) on the outer antenna, (b) on the inner antenna and (c) on the chip of RFID tags. (d) RSSI of the RFID tags shown by the tested screw locations.**

## 5.3 Experiment 7: Painting

One of the final and crucial stages in the manufacturing process of wooden items is the application of paint. However, there is a lack of certainty regarding the potential impact that a thin layer of paint commonly used on wooden items may have on the signal strength of embedded tags. This uncertainty is further complicated by the presence of moisture in certain types of paint, such as water-based paints. To address this knowledge gap, we conducted an experiment aimed at testing the effects of two different types of polyurethane wood finishes on the signals of embedded tags. Specifically, we tested a water-based polyurethane wood finish from Varathane and an oil-based polyurethane finish from Minwax. These two finishes were chosen based on their popularity and widespread use.

To conduct this study, we developed three identical copies of our prototype based on the findings from previous experiments. Each prototype consisted of a plywood substrate with a grid of  $3 \times 3$  RFID tags affixed to it. Additionally, we applied a 1mm thick veneer layer using wood glue onto the tags. To understand the impact of different paints on the RFID performance, we applied different types of paint to the two prototypes. One prototype was painted using water-based paint, another with oil-based paint, and the final one was left unpainted to serve as a baseline for comparison. Following the provided instructions, the surface of the prototypes was brush-painted, ensuring that an even layer of paint covered the entire surface. After painting, we allowed the paint to air dry for a period of 24 hours before conducting the test to measure the RSSI.

*Result.* The results of the study are presented in Figure 10. The findings indicate that there was a marginal decline in the RSSI when measured on painted surfaces in comparison to the baseline. Nonetheless, it is worth noting that despite this decline, the signals could still be consistently received in both water-based and oil-based painted conditions. These findings suggest that the presence of a light layer of paint does not significantly impede signal transmission. Therefore, it is unlikely that the performance of the sensor will be significantly affected by the presence of paint.

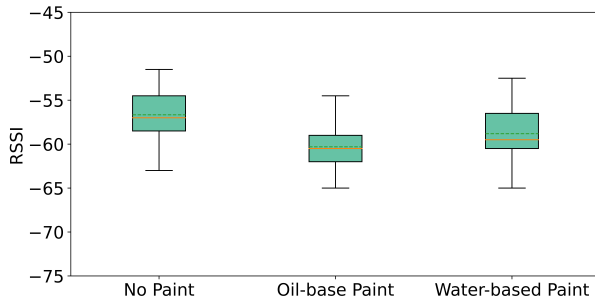


Figure 10: RSSI of the RFID tags shown by the tested painting conditions

## 6 FABRICATION

As previously noted, different categories of items may require varying tag densities in Tagnoo, depending on their intended applications. To achieve this, we fabricated several Tagnoo panels, each measuring  $122 \times 122$  cm in three types of tag densities: high ( $12 \times 12$  tags), medium ( $6 \times 6$  tags) and low density ( $4 \times 4$  tags). The distances between the tags for these different densities were set at 10 cm, 20 cm, and 30 cm, respectively, based on the findings from our prior experiments. Compared to standard plywood, the costs for these specialized panels rise by 8%, 2%, and 1% for the high, medium, and low densities, respectively. High-density Tagnoo panels are suitable for items that frequently come into contact with relatively small objects, such as desk surfaces. Medium-density panels, on the other hand, are designed for items that have less frequent interaction with small objects, like chair seats. The slightly lower tag density still provides adequate tracking capabilities for occasional contact with smaller items. Low-density panels, with their larger tag spacing, are intended for items that primarily come into contact with larger

objects, such as a floor. These panels provide sufficient tracking accuracy for larger objects while minimizing costs.

The fabrication process of the Tagnoo panels involved a four-step procedure. First, a unique material ID was assigned to the first half of the Electronic Product Code (EPC) for each tag. This assignment was carried out using a handheld RFID writer [27]. The material ID incorporates information about the tag’s density and sequence number in the material. The remaining bits within the EPC were reserved for potential future item ID assignments. Next, the RFID tags were attached to a plywood substrate with a thickness of 1.27cm. The alignment of these tags was executed in accordance with the desired density. Next, following our gluing strategy, a 1mm-thick veneer layer was firmly affixed on top of the tags. The glue was then left to dry for a period of 24 hours. Finally, to provide a protective and visually appealing finish, a layer of water-based finish was applied onto the surface of the panel. The structure of Tagnoo is illustrated in Figure 11.

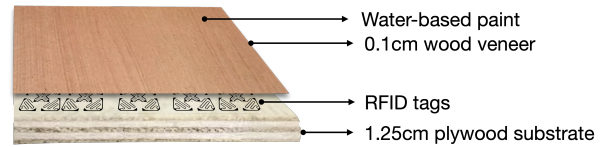


Figure 11: The structure of Tagnoo.

## 7 HARDWARE AND SOFTWARE IMPLEMENTATION

After setting up a space with items made of Tagnoo, our next step was to enable activity sensing within this environment. Thus, we designed a system that captured changes in tags’ RSSI values and fed them into a data processing pipeline along with machine learning algorithms to detect what happens in our experimental space. This section elaborates on the design and implementation aspects of our system.

### 7.1 Hardware

A typical sensing environment created using Tagnoo will have hundreds of tags. To scan these tags, we used an R420 UHF RFID reader in conjunction with two RFID antennas (Vulcan 262006). Each antenna was strategically positioned to cover an adjacent area, resulting in a combined coverage of approximately  $320 \times 250$  square centimetre. The antennas were mounted on the ceiling at a height of 200 cm above the ground. To effectively scan the environment, we switched between the antennas to read the tags within their coverage areas. In our implementation, the system operated at a sampling rate of approximately 1Hz. This sampling rate is sufficient for detecting the presence of static objects or simple user activities, such as sitting or standing on the floor. Note that higher sampling rates can be achieved by higher-end RFID readers or antennas, such as phased array antennas.

### 7.2 Data Processing Pipeline

In the data processing pipeline, the RSSI values of all the tags present in the environment were sampled and processed. To eliminate any ambient noise and account for baseline RF propagation, a

background profile was subtracted from the RSSI readings. This subtraction enabled a more precise representation of the interactions between the tags and objects or users. The background profile was established by taking the maximum of the RSSI readings from all the tags within a sliding window of 5 seconds. It was automatically updated when no objects or users were detected in the environment, indicating a period of inactivity, or when no tag reported a change in RSSI values exceeding a preset threshold (3 dB).

When an object or user interacts with a piece of furniture or the floor within the environment, our system detects their presence by analyzing the changes in RSSI values from the tags embedded in the furniture. This detection process involves summing up the changes in RSSI values and comparing them against a predetermined threshold (3 dB). If the summed change exceeds this threshold, the system identifies the presence of an object or user. Once the system detects this presence, it proceeds to monitor the standard deviation of the summed changes. The system waits until the standard deviation falls below a specific threshold (2 dB), within a 5-second time window. This indicates that the signal has stabilized and is ready for further processing. Next, the system smooths the RSSI values using a minimum filter because an object attenuates RF signals. We compute the relative changes in RSSI values for each tag, using the background profile as the reference for initial values. This process generates a series of RSSI data for each tag, arranged into a matrix based on the tag location within the sensing surface of furniture or floor. This data is then converted into a low-resolution image, which is then upscaled using a factor equal to the tag distance. For instance, the sensor data of a chair surface with a  $3 \times 3$  tag configuration, arranged at a medium density with a 20cm gap, is upscaled to a  $60 \times 60$  heatmap image. Similarly, the sensor data of a desk surface with a  $12 \times 6$  tag configuration, arranged at a high density with a 10cm gap, is upscaled to a  $120 \times 60$  heatmap image. Following this, the upscaled images from all the sensing surfaces in the environment are combined to form a single image, which can be used for training and evaluating our machine learning model.

### 7.3 Machine Learning

We employed a Convolutional Neural Network (CNN) classifier to tackle the classification of our sensor data, treating it as an image classification task. To avoid overfitting and optimize computational footprint and memory usage, we carefully designed our classifier with a lightweight architecture. The architecture of our model comprises four convolutional layers, with 8, 16, 32, and 64 filters, respectively, all utilizing a  $3 \times 3$  kernel size and Rectified Linear Unit (ReLU) activation functions. These convolutional layers were further augmented by max-pooling layers, which employed  $2 \times 2$  pooling windows to effectively reduce the spatial dimensions during the feature extraction process. The flattened features were then passed through a dense layer, consisting of 128 units, for subsequent classification.

We train over 100 epochs with a batch size of 16. Each epoch represents a complete pass through the entire training dataset, allowing the model to learn and adjust its weights. The selected batch size of 16 strikes a balance between computational load and frequency of weight updates, thereby facilitating smoother convergence. Throughout the training phase, the model undergoes

forward passes, generating predictions, and subsequently comparing them against the actual labels using categorical cross-entropy as the designated loss function. The backpropagation process follows, adjusting the model's weights to reduce error. The 'adam' optimizer aids in this by determining the learning rate and other parameters. At most, our lightweight CNN classifier contains approximately 2 million parameters, resulting in a model size of around 16 MB. This places our classifier in a similar range, in terms of size and complexity, as traditional classifiers, such as the Random Forest classifier, with a substantial depth (equivalent to approximately 32 trees).

## 8 CONSTRUCTING SMART ENVIRONMENTS USING TAGNOO

One of the primary goals for developing Tagnoo was to create an interactive material to facilitate the creation of smart environments with sensing capabilities by woodworkers or end-users who may not have traditional technical backgrounds. In order to demonstrate and validate the effectiveness of Tagnoo as a material, we organized a workshop involving two experienced woodworkers. The objective of the workshop was to construct a small office environment using our Tagnoo prototype.

The target environment for this workshop included a desk, chair, bookshelf, and a small section of floor. We employed high-density Tagnoo panels for the desktop, medium-density panels for the chair seat and shelves, and low-density panels for the floor. These panels could be used as a whole or cut into smaller sections to accommodate different furniture shapes and sizes. Considering that the majority of use cases for Tagnoo involve flat surfaces to detect the presence of daily objects, we focused on creating only flat surfaces of the target items using Tagnoo. Therefore, the legs for the desk and chair, as well as the vertical panel of the shelf, were purchased off the shelf.

*Procedure.* Before we started the workshop, the woodworkers were introduced to Tagnoo panels and were asked to work as a team to create the desk, chair, bookshelf, and floor. While suggestions regarding possible sizes for each item were given, the woodworkers were not restricted in making their own decisions during the crafting process. The final versions of these items were assembled using wood screws. The design of the desk incorporated a Tagnoo desktop, measuring  $122 \times 61$  cm. The chair had a Tagnoo seat, which measured  $55 \times 55$  cm. The floor comprised two Tagnoo boards, each measuring  $122 \times 91$  cm, resulting in a total floor area of  $122 \times 182$  cm. Finally, the bookshelf consisted of two Tagnoo shelves, each measuring  $80 \times 28$  cm. Note that the final bookshelf comprised a total of three shelves. One of the shelves was intentionally included without sensing capability and was positioned between the tagged shelves. This arrangement aimed to investigate the potential for sensing events occurring on the untagged shelf from the tagged shelves. During the task, the participants decided to distribute the various responsibilities among themselves. One participant took charge of the cutting process, while another participant handled the assembly. To facilitate the cutting of the desired pieces, a table saw was provided, and a sander was used after cutting to ensure the smoothness of the newly cut edges. After the completion of the cutting tasks, the second participant completed the assembly task.



This task involved drilling pilot holes in the predetermined locations and subsequently fastening the pieces together using screws, thereby finalizing the furniture assembly process. Upon completion, the finished furniture and floors were positioned below the RFID antennas.

*Result.* The participants followed their usual workflow during the task and successfully completed creating the target environment in less than an hour. Figure 12 shows the outcomes of their work and the arrangement of the items in a 320 cm by 250 cm open space. Note that placing all the furniture on the floor resulted in limited open space for user activities. Therefore, we decided to position the furniture outside of the floor area. To gain insight into the number of embedded tags within the finished environment, we examined the furniture and the floor. Our findings revealed the presence of  $3 \times 3$ ,  $6 \times 12$ , and  $4 \times 6$  tags embedded within the seat, desktop, and floor, respectively. Furthermore, one of the shelves contained  $1 \times 4$  tags, while the other shelf had  $2 \times 4$  tags. We also examined the functionality of the tags and found that some of the tags had malfunctioned due to the cutting process. Specifically, inside the shelf, including a grid of  $2 \times 4$  tags, only one row of these tags remained operational. This particular shelf was found in the lower position of the bookshelf. In contrast, no broken tags were found in the rest of the environment. It is worth noting that the RFID tags operate independently of each other. Therefore, any broken tags, whether damaged during the cutting or screwing processes, become unreadable but do not negatively impact the readability of the other tags within the environment.

Concerning user experience, the participant responsible for the cutting operation stated that the Tagnoo panels exhibited comparable stiffness and elasticity to regular plywood. They observed no apparent differences while cutting it. However, he did encounter an issue with the edges of the plywood, which exhibited uneven tear-out and splintering after the cutting process. This particular issue is not observed with regular plywood. As a result, further finishing was required to address this problem. This issue can primarily be attributed to the manual attachment of the veneer layer and could be easily resolved using higher-end professional tools. They did not perceive any noticeable difference during the pre-hole and assembly processes.

## 9 EVALUATION

We conducted an experiment to measure the sensing performance of the smart environment that was created in the workshop. The goal of this experiment was to measure the accuracy of the system in detecting the presence of objects and user activities as described in the previous section.

### 9.1 Objects and Activities

In our experiment, we tested a total of 18 objects and user activities, primarily selected from the scenario described in Section 3 (Figure 13). Specifically, we tested 8 events on the desk, including the presence of a 16-inch laptop, a user typing on the laptop, a chocolate bar, a craft hardboard, a book, a glass lunchbox, the glass lunchbox filled with rice, and a backpack. For the bookshelf, we conducted tests on 4 events, which involved placing a book on the top, middle, and bottom shelf, as well as having a user standing next to the shelf. On the chair, we tested 3 events, which included

a user sitting on the chair, an empty backpack placed on the chair, and the same backpack with the 16-inch laptop inside. Lastly, on the floor, we tested 3 events, which involved a user sitting, standing, and lying on the floor. The selection of object and event locations was based on their natural and logical occurrence within the tested environment.

### 9.2 Participants

Ten right-handed participants were recruited for the user activities, including typing on a laptop, sitting on a chair, standing next to a shelf, and various positions on the floor (standing, lying, and sitting). The participants had an average age of 22 years, with five males and five females. A volunteer carried out data collection for the objects.

### 9.3 Data Collection

A volunteer was invited to collect the training data for the machine learning model. The volunteer was asked to place each of the tested objects inside the sensing area of each item in a random location, orientation, and order. No other instruction was given in terms of how the objects should be presented to the sensor.

For the data on user activities, participants were instructed to carry out each activity ten times without any restrictions on their body position or orientation within the sensor. For instance, when typing on the laptop, participants placed the laptop anywhere on the table and proceeded with typing. To simulate searching for books near the bookshelf, participants varied the trials by choosing different locations in front of the shelf. For activities performed on the floor, participants stood and sat at different locations with random body orientations. When lying on the floor, half of the trials had the participant's head positioned on one end, while the other half had the head positioned at the opposite end. The raw data confirmed that objects and activities occurred across a wide variety of locations and orientations, including those in close proximity to the center, as well as those that took place near the edges or corners of the sensors.

As described in the Data Processing Pipeline section, the sensor data obtained from the entire environment, including the table, chair, bookshelf, and floor, was combined into a single heatmap image for model training and testing.

### 9.4 Results

In this section, we present the results of our study on the recognition accuracy of Tagnoo. Particularly, we present the system's performance by comparing the use of a single general model for the entire environment with the use of individual models for each item in isolation.

*9.4.1 General model accuracy* We first evaluated the sensing accuracy of our system by treating all furniture and the floor as a unified environment as illustrated in Figure 14. We employed a two-fold cross-validation using a model trained on all the data collected from the desk, chair, bookshelf, and floor. The results of our evaluation demonstrated that our system achieved an accuracy of 93.9% (SD = 5.9). Examining the confusion matrix of the result revealed that out of the 18 tested objects and activities, 14 of them achieved an accuracy higher than 90%. This finding is particularly encouraging

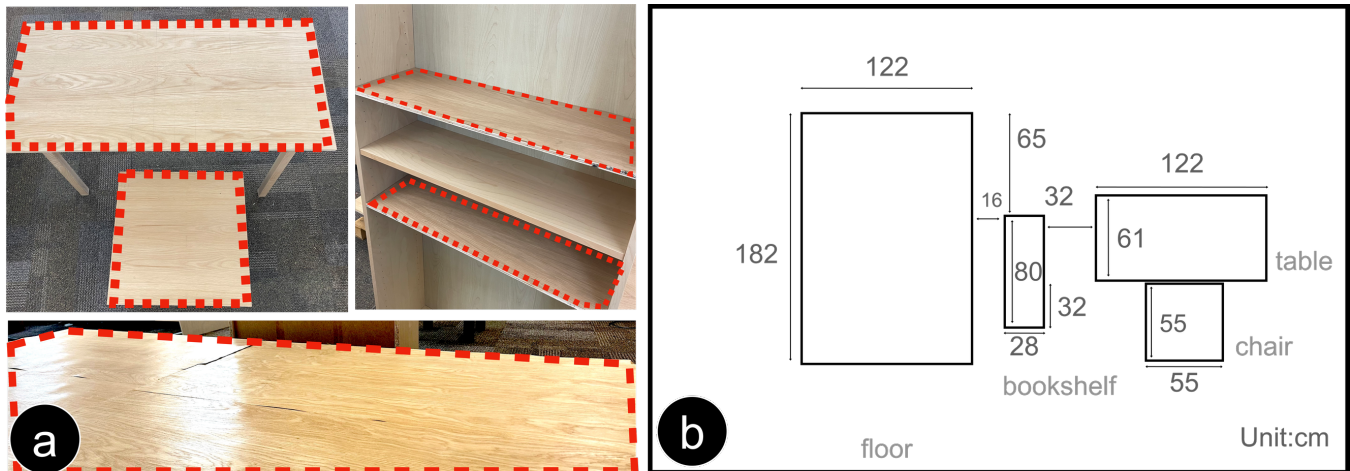


Figure 12: (a) A desk, chair, bookshelf, and floor were constructed in the workshop. The furniture and floor surfaces circled in red are made of Tagnoo. (b) The floor layout shows the arrangement of these items.



Figure 13: The full list of tested objects and activities. The events tested on the desk include (a) a 16-inch laptop, (b) a user typing on the laptop, (c) a chocolate bar, (d) a craft hardboard, (e) a book, a glass lunchbox, (f) the glass lunchbox filled with rice, and (h) a backpack on the table. The events tested on the bookshelf include (i) a book on the top shelf, (j) a book on the middle shelf, (k) a book on the bottom shelf, and (l) a user standing next to the shelf. The events tested on the chair include (n) a user sitting on the chair, (m) an empty backpack placed on the chair, and (o) the same backpack with the 16-inch laptop inside. Lastly, the events tested on the floor include (p) a user sitting on the floor, (q) a user standing on the floor, and (r) a user lying on the floor.

as it suggests that our system is capable of accurately recognizing and distinguishing between objects that possess similar shapes but differ in material composition. For instance, objects such as a book, an empty lunchbox, and a lunchbox filled with rice, all of which share a rectangular shape, were successfully identified by our system with relatively high accuracy.

On the contrary, our result revealed that the majority of misclassifications occurred when the system attempted to determine the specific shelf where a book was positioned. This can be attributed to the fact that the sensor data collected from the top and bottom shelves alone were inadequate for accurately identifying an object placed on the middle shelf, which was not augmented with Tagnoo. Furthermore, we observed that user movements on the floor also caused some confusion for the system. This can likely be attributed to the diverse body shapes of our participants, resulting in varying

levels of obstruction to the RF signal. As a consequence, our model faced difficulties in accurately discerning the specific activity being performed by the users.

**9.4.2 Item-specific model accuracy** In addition to assessing the overall accuracy of our general model, we measured sensing accuracy for each individual piece of furniture and the floor. To do this, we performed a two-fold cross-validation for each model trained using the specific data collected for each item while excluding data from the remaining environment. The results also revealed a high level of accuracy for each item, with the table achieving 95.3% accuracy (SD = 4), the bookshelf achieving 91.2% accuracy (SD = 6.8), the chair achieving 94.2% accuracy (SD = 9.0), and the floor achieving 91.6% accuracy (SD = 4.7). The corresponding confusion matrix can be found in Figure 15.

	a	b	c	d	e	f	g	h	i	j	k	l	n	m	o	p	q	r
Table	a. laptop	100	0	0	0	0	0	0	0	0	0	0	0	0	0	0	0	0
	b. typing on laptop	0	100	0	0	0	0	0	0	0	0	0	0	0	0	0	0	0
	c. chocolate bar	0	0	98	0	0	0	0	0	0	0	0	0	0	0	0	0	2
	d. craft hardboard	0	0	0	100	0	0	0	0	0	0	0	0	0	0	0	0	0
	e. book	0	0	0	1	98	0	1	0	0	0	0	0	0	0	0	0	0
	f. glass lunchbox	0	0	0	0	0	100	0	0	0	0	0	0	0	0	0	0	0
	g. glass lunchbox with rice	0	0	1	0	4	0	94	1	0	0	0	0	0	0	0	0	0
	h. backpack	4	0	3	2	0	0	0	91	0	0	0	0	0	0	0	0	0
Book shelf	i. book on top shelf	0	0	0	0	0	0	0	87	7	6	0	0	0	0	0	0	0
	j. book on mid shelf	0	0	0	0	0	0	0	3	92	5	0	0	0	0	0	0	0
	k. book on bot shelf	0	0	0	0	0	0	0	10	11	79	0	0	0	0	0	0	0
	l. stand next to bookshelf	0	0	0	0	0	0	0	1	0	3	96	0	0	0	0	0	0
Chair	n. sitting on chair	0	0	0	0	0	0	0	0	0	0	0	97	0	3	0	0	0
	m.backpack	0	0	0	0	0	0	0	0	0	0	0	0	100	0	0	0	0
	o. backpack with laptop	0	0	0	0	0	0	0	0	0	0	0	1	7	92	0	0	0
Floor	p. sitting on floor	0	0	0	0	0	0	0	0	0	0	0	0	0	0	89	10	1
	q. standing on floor	0	0	0	0	0	0	0	0	0	0	0	0	0	0	12	88	0
	r. lying on floor	0	0	0	0	0	0	0	0	0	0	0	0	0	0	7	3	90

Figure 14: The confusion matrix of the general model accuracy.

	a	b	c	d	e	f	g	h	i	j	k	l	n	m	o	p	q	r	
Table	a. laptop	92	1	0	4	0	0	0	3										
	b. typing on laptop	5	94	0	0	0	0	0	1										
	c. chocolate bar	0	0	96	0	1	0	2	1										
	d. craft hardboard	0	0	0	100	0	0	0	0										
	e. book	0	0	0	0	96	2	0	2										
	f. glass lunchbox	0	0	0	0	0	100	0	0										
	g. glass lunchbox with rice	1	0	0	0	1	0	97	1										
	h. backpack	2	0	6	2	1	0	1	88										
Book shelf	i. book on top shelf								94	2	4	0							
	j. book on mid shelf								2	89	8	0							
	k. book on bot shelf								3	14	83	0							
	l. stand next to bookshelf								1	0	0	99							
Chair	n. sitting on chair												100	0	0	8			
	m.backpack												0	81	11	9			
	o. backpack with laptop												0	4	96	0			
Floor	l. stand next to bookshelf												0	0	0	100			
	p. sitting on floor																88	9	3
	q. standing on floor																3	97	0
	r. lying on floor																4	6	90

Figure 15: The confusion matrix of the item-specific model accuracy.

The results of the study indicate instances where the sensing accuracy was compromised when a complete picture of sensor data from the surrounding environment was not available. Specifically, the identification of joint events occurring across different pieces of furniture was hindered. For instance, when the data from the chair is excluded from the model, there is a misclassification of typing on the laptop, often confusing it with the laptop being placed solely on the table. This misclassification can be attributed to the absence of data regarding someone sitting in the chair, causing the system to inaccurately attribute the activity solely to the table. To further investigate the influence of missing the surrounding environment, we intentionally incorporated the data collected on the chair with participants standing between the chair and the bookshelf. Unlike

in the general model, the data collected on the bookshelf was excluded. The analysis revealed that the model frequently confuses situations where only a bag is present on the chair with situations where a person is standing between the chair and the shelf. This finding suggests that when developing a model for individual smart items, a more comprehensive set of test scenarios should be considered to minimize false positives. Interestingly, we did not observe any significant increase or decrease in average accuracy for the bookshelf and floor. This can be attributed to the fact that in the tested environment, the events that took place on these items were more dedicated to the items themselves.

## 10 LIMITATION AND FUTURE WORK

In this section, we acknowledge the limitations of our study and provide an overview of our key findings. We also explore the implications of these insights and suggest potential avenues for future research to address unanswered questions and expand on our findings.

### 10.1 Detecting and Locating Multiple Objects or Users

Our current implementation relies on a simple machine learning algorithm to detect the presence of an object and user by analyzing the RSSI values of the tag grid. While this approach works well for simple scenes, it may not be suitable for more complex scenarios involving the simultaneous locating and tracking of multiple objects or users, particularly in the presence of multi-path signals. To tackle this challenge, utilizing a deep learning model might offer a more robust solution [60, 100]. However, incorporating deep learning models into our system is not without its difficulties. One major concern is the potential interference between objects, which can hinder the accurate sensing of material information. For instance, when two objects are in close proximity, their RSSI patterns may overlap, leading to difficulties in distinguishing between them. This overlap poses a significant challenge that needs to be addressed. One possible approach to address this challenge is by employing a super resolution network model [38, 70]. This approach has the potential to generate higher-resolution data by uncovering hidden information within the low-resolution data. By enhancing the resolution of the data, it may become easier to distinguish between overlapping RSSI patterns and accurately identify individual objects or users. However, it is important to note that further exploration and validation are required to determine the effectiveness of this approach.

### 10.2 Latency

Our current research primarily centers on material-related concerns. As a result, certain technical improvements have been omitted from the scope of this study. A notable technical limitation is the sampling rate limitation of our current system, which poses a challenge to work effectively in an environment with a higher number of RFID tags or to accurately recognize fine-grained user activities, such as writing and erasing on a desk. To address this limitation, we propose two potential solutions: adaptive sampling and beamforming. Adaptive sampling is a technique that strategically allocates computational resources to specific areas of interest while minimizing focus on peripheral regions. In our context, this means that we can prioritize the sampling of RFID tags that are closer to the occurrence of an event of interest. This approach can be achieved during the tag singulation process, where only the tag corresponding to the serial string provided by the system is activated. By selectively sampling tags in proximity to the event, we can improve the sampling rate of the system. Another promising solution is beamforming, which involves directing RF signals in specific directions. This reduces conflict resolution time, as fewer tags are present in the targeted scan areas. Additionally, beamforming enables the coordination of multiple RFID readers to scan various regions simultaneously,

thereby enhancing the overall sampling rate. By combining adaptive sampling and beamforming techniques, we can significantly increase the RFID reading rate and potentially achieve fine-grained activity recognition in a larger-scale environment.

### 10.3 Sensing Beyond a Fixed Environment

Our current sensing approach operates effectively in a fixed environment where the furniture's location remains constant. However, in real-world scenarios, it is common for changes to be made regarding the arrangement and layout of household items within the environment. Additionally, the location or orientation of the household items may also be subject to change, which can affect the sensor readings and subsequently impact recognition accuracy. To address this issue, it is essential to develop a generalizable model that takes into account the arrangement layouts of items and the locations of the RFID antenna. This information can be manually provided by workers during the construction of the environment, or it can be automatically estimated using RFID readers equipped with localization techniques [45, 66, 109], such as Impinj xArray Gateway RFID Reader [28]. By incorporating this information, the system could potentially accommodate the changes within the smart environment. Nevertheless, this approach necessitates careful investigation in the future to validate its effectiveness.

### 10.4 Capabilities Beyond RF Sensing

The focus of our research revolves around computational materials that possess sensing, computing, and communication capabilities. We developed Tagnoo as an example of such a material due to its batteryless nature, cost-effectiveness, and resilience against fabrication operations. Tagnoo's inherent computing and communication abilities make it a promising candidate for easy integration with additional functionalities beyond RF sensing. One possible augmentation for RFID tags is capacitive sensing. Recent studies have explored the potential of enhancing RFID tags with capacitive sensing capabilities [36, 90]. This additional feature expands the range of applications that can be addressed by Tagnoo. Moreover, the memory capacity of RFID tags can be leveraged to enable novel applications. For instance, objects created using Tagnoo can store meta-information within the memory of the RFID tags. This information can then be accessed and manipulated through augmented reality AR interfaces. Such an integration would enable users to interact with the physical environment in a more immersive and dynamic manner, bridging the gap between the physical and virtual worlds.

### 10.5 Comparison with RF Sensing Using mmWave Radar

It is worth noting that mmWave radar sensors offer similar sensing capabilities but through the use of electromagnetic waves for capturing the three-dimensional geometry of an environment. These sensors can be likened to "cameras" that operate using high-frequency waves. One distinct advantage of mmWave radar is its ability to function effectively in various environmental conditions, including low light or obstructed environments such as walls or fog. However, mmWave radar tends to exhibit lower sensing resolution when the sensing range is long [38]. In contrast to mmWave



radar, the approach adopted by Tagnoo leverages the density and strategic placement of RFID tags in order to optimize sensing resolution. While our current implementation may not offer an extended sensing range, this limitation can be overcome by incorporating higher-end RFID readers and antennas [26]. Moreover, mmWave radar systems often prove to be expensive and power-intensive, particularly for long-range applications, which contradicts the goals of computational materials. In contrast, our system provides a more energy-efficient and cost-effective solution. At present, we are actively exploring methods to extend the reading range of Tagnoo without compromising the sensing resolution. By doing so, we aim to enhance the overall effectiveness and functionality of our system.

## 10.6 Recycle of Tagnoo

The integration of RFID tags in plywood poses new challenges in the recycling process. If these tags are not disassembled properly, they could contaminate recycled wood streams or emit harmful substances during incineration. To address these issues, our future research will focus on a two-step solution. Firstly, we plan to refine the design of Tagnoo to incorporate an easy-to-dismantle mechanism. Our objective is to develop a design that guides users to easily access and remove the RFID tags before initiating the recycling process. Secondly, we aim to develop spectral sensing and analysis tools that can be deployed at recycling centers. These tools will enable the seamless identification and separation of Tagnoo products from regular plywood. This way, we can accurately distinguish Tagnoo products, based on their unique characteristics and ensure that different components of Tagnoo receive the specialized recycling treatment it require.

## 10.7 Upcycling

Tagnoo offers a unique opportunity for the upcycling of furniture and household items, transforming them into new creations that serve different purposes. Similar to existing furniture, Tagnoo can be repurposed into various items, granting them a second life. However, what distinguishes Tagnoo is its digital properties, which can be inherited by these new items. This inheritance enables the upcycled items to become interactive and seamlessly integrate into the smart ecosystem.

## 10.8 Privacy Control

Users may have a desire to disable the sensing functionality of Tagnoo in certain situations. Although the entire smart environment can be deactivated by turning off the RF antennas and readers, selectively disabling a specific item composed of Tagnoo furniture presents a challenge at present. To tackle this issue, one potential solution is to design a user-friendly toolkit that enables users to easily shield the tags embedded within the plywood, by utilizing a metallic cover. Another potential solution involves the creation of methods to enable the RFID reader to bypass the group of tags within a desired item.

## 10.9 End-User Tools

End-user tools play a crucial role in the democratization of computational material. In our future research, we plan to develop end-user tools that will facilitate the seamless configuration of tag positions

and distributions within diverse material designs. Additionally, we aim to design tools that will ease the machine learning pipeline, guiding users through the process of data collection, model training, and implementation in real-world scenarios. With these tools, our objective is to empower end users, irrespective of their technical background, with the capability to customize the functionality of their Tagnoo-enhanced objects to meet their specific needs and preferences.

## 11 Conclusion

Tagnoo addresses the significant challenges associated with the implementation of room-scale smart environments using computational materials. Not only does Tagnoo offer a cost-effective and battery-free solution, but it also seamlessly integrates into existing woodworking workflows, enabling woodworkers to easily create smart furniture and infrastructure. By overcoming obstacles related to battery consumption, cost, material form factor, and damage resistance, Tagnoo paves the way for the widespread adoption of smart environments that seamlessly blend into our physical surroundings. The impact of this research extends beyond the scope of this paper. It presents exciting possibilities for a future where everyday materials can actively sense and respond to user activities. This work has the potential to serve as a practical solution to revolutionize homes and workplaces, blurring the boundary between the digital and physical worlds.

## References

- [1] 2023. All Sales Final - Omni-ID Exo 750 RFID Tag. <https://www.atlasrfidstore.com/all-sales-final-omni-id-exo-750-rfid-tag>
- [2] 2023. Amazon Product B07MD7CK5D. [https://www.amazon.ca/gp/product/B07MD7CK5D/ref=ppx\\_yo\\_dt\\_b\\_asin\\_title\\_o06\\_s00?ie=UTF8&psc=1](https://www.amazon.ca/gp/product/B07MD7CK5D/ref=ppx_yo_dt_b_asin_title_o06_s00?ie=UTF8&psc=1)
- [3] 2023. Avery Dennison AD-301r6-P UHF RFID Wet Inlay Monza R6-P. <https://www.atlasrfidstore.com/avery-dennison-ad-301r6-p-uhf-rfid-wet-inlay-monza-r6-p>
- [4] 2023. Avery Dennison AD-321r6-P UHF RFID Wet Inlay Monza R6-P. <https://www.atlasrfidstore.com/avery-dennison-ad-321r6-p-uhf-rfid-wet-inlay-monza-r6-p>
- [5] 2023. Avery Dennison Smartrac AD-237r6-P UHF RFID Wet Inlay Monza R6-P. <https://www.atlasrfidstore.com/avery-dennison-smartrac-ad-237r6-p-uhf-rfid-wet-inlay-monza-r6-p>
- [6] 2023. Avery Dennison Smartrac Dogbone RFID Wet Inlay M750. <https://www.atlasrfidstore.com/avery-dennison-smartrac-dogbone-rfid-wet-inlay-m750>
- [7] 2023. Beontag BUHRER P60 RFID Wet Inlay M750. <https://www.atlasrfidstore.com/beontag-buhrer-p60-rfid-wet-inlay-m750>
- [8] 2023. Beontag F62 RFID Paper Tag Monza R6-P. <https://www.atlasrfidstore.com/beontag-f62-rfid-paper-tag-monza-r6-p/>
- [9] 2023. Confidex 4x6 Crosswave Classic UHF RFID Label Monza 4E. <https://www.atlasrfidstore.com/confidex-4x-6-crosswave-classic-uhf-rfid-label-monza-4e>
- [10] 2023. Confidex Steelwave Micro 2 RFID Tag. <https://www.atlasrfidstore.com/confidex-steelwave-micro-2-rfid-tag>
- [11] 2023. HID iQ Pro 400P HT M730 UHF Label. <https://www.atlasrfidstore.com/hid-iq-pro-400p-ht-m730-uhf-label>
- [12] 2023. HID Slimflex UHF RFID Tag M730. <https://www.atlasrfidstore.com/hid-slimflex-uhf-rfid-tag-m730>
- [13] 2023. Impinj-H47 Monza-4E UHF PET Label. [https://www.amazon.ca/gp/product/B01778XKUY/ref=ppx\\_yo\\_dt\\_b\\_asin\\_title\\_o08\\_s00?ie=UTF8&psc=1](https://www.amazon.ca/gp/product/B01778XKUY/ref=ppx_yo_dt_b_asin_title_o08_s00?ie=UTF8&psc=1)
- [14] 2023. Vulcan RFID Arrow UHF RFID White Wet Inlay NXP UCODE 8. <https://www.atlasrfidstore.com/vulcan-rfid-arrow-uhf-rfid-white-wet-inlay-nxp-ucode-8>
- [15] 2023. Vulcan RFID Custom Credential Tag. <https://www.atlasrfidstore.com/vulcan-rfid-custom-credential-tag>
- [16] 2023. Vulcan RFID Custom Universal Mini Asset Tag. <https://www.atlasrfidstore.com/vulcan-rfid-custom-universal-mini-asset-tag>
- [17] 2023. Vulcan RFID Embeddable RFID Wire Tag. <https://www.atlasrfidstore.com/vulcan-rfid-embeddable-rfid-wire-tag>
- [18] 2023. Vulcan RFID Fire UHF RFID White Wet Inlay NXP UCODE 8. <https://atlasrfidstore.com/vulcan-rfid-fire-uhf-rfid-white-wet-inlay-nxp-ucode-8>

- [19] 2023. Vulcan RFID Flame UHF RFID White Wet Inlay M730. <https://www.atlasrfidstore.com/vulcan-rfid-flame-uhf-rfid-white-wet-inlay-m730>
- [20] 2023. Vulcan RFID Label 4 x 2 / 4 x 6 for Zebra and Sato Industrial RFID Printers. <https://www.atlasrfidstore.com/vulcan-rfid-label-4-x-2-4-x-6-for-zebra-and-sato-industrial-rfid-printers>
- [21] 2023. Vulcan RFID Torch UHF RFID White Wet Inlay M730. <https://www.atlasrfidstore.com/vulcan-rfid-torch-uhf-rfid-white-wet-inlay-m730>
- [22] 2023. Xerafy Pico On Plus RFID Tag. <https://www.atlasrfidstore.com/xerafy-pico-on-plus-rfid-tag>
- [23] 2023. YARONGTECH Alien RFID Tag. [https://www.amazon.ca/YARONGTECH-ISO18000-6C-Alien-73-5x21-2mm-Adhesive/dp/B07BZHKG3/ref=sr\\_1\\_3?crid=12FVY6S2ETPTZ&keywords=UHF+RFID+tags&qid=1701150477&s=electronics&prefix=uhf+rfid+tags%2Celectronics%2C115&sr=1-3](https://www.amazon.ca/YARONGTECH-ISO18000-6C-Alien-73-5x21-2mm-Adhesive/dp/B07BZHKG3/ref=sr_1_3?crid=12FVY6S2ETPTZ&keywords=UHF+RFID+tags&qid=1701150477&s=electronics&prefix=uhf+rfid+tags%2Celectronics%2C115&sr=1-3)
- [24] 2023. Zebra Silverline Blade II RFID Tag by Confidex M730. <https://www.atlasrfidstore.com/zebra-silverline-blade-ii-rfid-tag-by-confidex-m730>
- [25] Aug 2023. Impinj E62 UHF RFID. [https://rfid.atlasrfidstore.com/hubfs/1\\_Tech\\_Spec\\_Sheets/CCR/ATLAS%20CCR%20E62%20RFID%20White%20Wet%20Inlay%20\(Monza%20R6-P\).pdf](https://rfid.atlasrfidstore.com/hubfs/1_Tech_Spec_Sheets/CCR/ATLAS%20CCR%20E62%20RFID%20White%20Wet%20Inlay%20(Monza%20R6-P).pdf)
- [26] Aug 2023. R787 UHF RFID Reader 25m Long Range Outdoor IP67 12dbi Antenna. <https://www.yanzeo.com/rfid-write-reader/uhf-rfid-readers/r787-uhf-rfid-reader-25m-long-range-outdoor-ip67-12dbi-antenna-usb-rs232-rs485-wiegand-output-uhf-integrated-reader.html>
- [27] Aug 2023. Thincol RFID Writer. [https://www.amazon.ca/gp/product/B08RDXGNGF/ref=ppx\\_yo\\_dt\\_b\\_asin\\_title\\_o05\\_s00?ie=UTF8&psc=1](https://www.amazon.ca/gp/product/B08RDXGNGF/ref=ppx_yo_dt_b_asin_title_o05_s00?ie=UTF8&psc=1)
- [28] Nov 2023. Impinj xArray Gateway RFID Reader. <https://www.atlasrfidstore.com/impinj-xarray-gateway-rfid-reader/>
- [29] Gregory D. Abowd. 2020. The Internet of Materials: A Vision for Computational Materials. *IEEE Pervasive Computing* 19, 2 (2020), 56–62. <https://doi.org/10.1109/MPRV.2020.2982475>
- [30] Fadel Adib, Hongzi Mao, Zachary Kabelac, Dina Katabi, and Robert C. Miller. 2015. Smart Homes That Monitor Breathing and Heart Rate. In *Proceedings of the 33rd Annual ACM Conference on Human Factors in Computing Systems* (Seoul, Republic of Korea) (CHI '15). Association for Computing Machinery, New York, NY, USA, 837–846. <https://doi.org/10.1145/2702123.2702200>
- [31] Nicholas Akinyokun and Vanessa Teague. 2017. Security and Privacy Implications of NFC-Enabled Contactless Payment Systems. In *Proceedings of the 12th International Conference on Availability, Reliability and Security* (Reggio Calabria, Italy) (ARES '17). Association for Computing Machinery, New York, NY, USA, Article 47, 10 pages. <https://doi.org/10.1145/3098954.3103161>
- [32] Alejandro Alanis, Gerald DeJean, Ran Gilad-Bachrach, and Dimitrios Lymberopoulos. 2014. 3D Gesture Recognition Through RF Sensing. Technical Report MSR-TR-2014-81. <https://www.microsoft.com/en-us/research/publication/3d-gesture-recognition-through-rf-sensing/>
- [33] Nivedita Arora and Gregory D. Abowd. 2018. ZEUSSS: Zero Energy Ubiquitous Sound Sensing Surface Leveraging Triboelectric Nanogenerator and Analog Backscatter Communication. In *Adjunct Proceedings of the 31st Annual ACM Symposium on User Interface Software and Technology* (Berlin, Germany) (UIST '18 Adjunct). Association for Computing Machinery, New York, NY, USA, 81–83. <https://doi.org/10.1145/3266037.3266108>
- [34] Nivedita Arora, Ali Mirzazadeh, Injoon Moon, Charles Ramey, Yuhui Zhao, Daniela C. Rodriguez, Gregory D. Abowd, and Thad Starner. 2021. MARS: Nano-Power Battery-Free Wireless Interfaces for Touch, Swipe and Speech Input. In *The 34th Annual ACM Symposium on User Interface Software and Technology* (Virtual Event, USA) (UIST '21). Association for Computing Machinery, New York, NY, USA, 1305–1325. <https://doi.org/10.1145/3472749.3474823>
- [35] Nivedita Arora, Steven L. Zhang, Fereshth Shahmiri, Diego Osorio, Yi-Cheng Wang, Mohit Gupta, Zhengjun Wang, Thad Starner, Zhong Lin Wang, and Gregory D. Abowd. 2018. SATURN: A Thin and Flexible Self-Powered Microphone Leveraging Triboelectric Nanogenerator. *Proc. ACM Interact. Mob. Wearable Ubiquitous Technol.* 2, 2, Article 60 (jul 2018), 28 pages. <https://doi.org/10.1145/3214263>
- [36] Carol L. Baumbauer, Matthew G. Anderson, Jonathan Ting, Akshay Sreekumar, Jan M. Rabaey, Ana C. Arias, and Arno Thielsens. 2020. Printed, flexible, compact UHF-RFID sensor tags enabled by hybrid electronics. *Scientific Reports* 10, 1 (Oct. 2020), 16543. <https://doi.org/10.1038/s41598-020-73471-9>
- [37] Muhammad Umair Bukhari, Kashif Riaz, Tauseef Tauqeer, and Mameen Sajid. 2019. Simple and low cost triboelectric nanogenerator (TEG) for resource limited environment. In *2019 International Conference on Robotics and Automation in Industry* (ICRAI). 1–4. <https://doi.org/10.1109/ICRAI47710.2019.8967354>
- [38] Hsin-Yuan Chang, Yi-Yan Chen, and Wei-Ho Chung. 2022. RangeSRN: Range Super-Resolution Network Using mmWave FMCW Radar. In *GLOBECOM 2022 - 2022 IEEE Global Communications Conference*. 1–6. <https://doi.org/10.1109/GLOBECOM48099.2022.10000943>
- [39] Zhe Chen, Chao Cai, Tianyue Zheng, Jun Luo, Jie Xiong, and Xin Wang. 2023. RF-Based Human Activity Recognition Using Signal Adapted Convolutional Neural Network. *IEEE Transactions on Mobile Computing* 22, 1 (2023), 487–499. <https://doi.org/10.1109/TMC.2021.3073969>
- [40] Gabe Cohn, Daniel Morris, Shwetak N. Patel, and Desney S. Tan. 2011. Your Noise is My Command: Sensing Gestures Using the Body as an Antenna. In *Proceedings of the SIGCHI Conference on Human Factors in Computing Systems* (Vancouver, BC, Canada) (CHI '11). Association for Computing Machinery, New York, NY, USA, 791–800. <https://doi.org/10.1145/1978942.1979058>
- [41] Diane Cook and Sajal Das. 2004. *Smart Environments: Technology, Protocols and Applications* (Wiley Series on Parallel and Distributed Computing). Wiley-Interscience, USA.
- [42] Lei Cui, Zonghua Zhang, Nan Gao, Zhaozong Meng, and Zhen Li. 2019. Radio Frequency Identification and Sensing Techniques and Their Applications—A Review of the State-of-the-Art. *Sensors* 19, 18 (Sept. 2019), 4012. <https://doi.org/10.3390/s19184012>
- [43] Stijn Denis, Rafael Berkvens, and Maarten Weyn. 2019. A Survey on Detection, Tracking and Identification in Radio Frequency-Based Device-Free Localization. *Sensors* 19, 23 (Dec. 2019), 5329. <https://doi.org/10.3390/s19235329>
- [44] Maloy Kumar Devnath, Avijoy Chakma, Mohammad Saeid Anwar, Emon Dey, Zahid Hasan, Marc Conn, Biplab Pal, and Nirmalya Roy. 2023. A Systematic Study on Object Recognition Using Millimeter-wave Radar. In *2023 IEEE International Conference on Smart Computing (SMARTCOMP)*. 57–64. <https://doi.org/10.1109/SMARTCOMP58114.2023.00025>
- [45] Alseny Diallo, Zaixin Lu, and Xinghui Zhao. 2019. Wireless Indoor Localization Using Passive RFID Tags. *Procedia Computer Science* 155 (2019), 210–217. <https://doi.org/10.1016/j.procs.2019.08.031>
- [46] Peter Dickman, Gareth P. McSorley, Jim Liddell, John Glen, and Jim Green. 2007. The Design and Development of an RFID-Enabled Asset Tracking System for Challenging Environments. *Int. J. Internet Protoc. Technol.* 2, 3/4 (dec 2007), 232–239. <https://doi.org/10.1504/IJIPT.2007.016223>
- [47] Chao Feng, Jie Xiong, Liqiong Chang, Fuwei Wang, Ju Wang, and Dingyi Yang. 2021. RF-Identity: Non-Intrusive Person Identification Based on Commodity RFID Devices. *Proc. ACM Interact. Mob. Wearable Ubiquitous Technol.* 5, 1, Article 9 (mar 2021), 23 pages. <https://doi.org/10.1145/3448101>
- [48] Jun Gong, Yu Wu, Lei Yan, Teddy Seyed, and Xing-Dong Yang. 2019. Tensitive: Contextual interactions on interactive fabrics with inductive sensing. In *Proceedings of the 32nd Annual ACM Symposium on User Interface Software and Technology*. 29–41.
- [49] Jian Gong, Xinyu Zhang, Kaixin Lin, Ju Ren, Yaoxue Zhang, and Wenxun Qiu. 2021. RF Vital Sign Sensing under Free Body Movement. *Proc. ACM Interact. Mob. Wearable Ubiquitous Technol.* 5, 3, Article 101 (sep 2021), 22 pages. <https://doi.org/10.1145/3478090>
- [50] Sidhant Gupta, Matthew S. Reynolds, and Shwetak N. Patel. 2010. ElectriSense: Single-point Sensing Using EMI for Electrical Event Detection and Classification in the Home. In *Proceedings of the 12th ACM International Conference on Ubiquitous Computing* (Copenhagen, Denmark) (UbiComp '10). ACM, New York, NY, USA, 139–148. <https://doi.org/10.1145/1864349.1864375>
- [51] Unsoo Ha, Junshan Leng, Alaa Khaddaj, and Fadel Adib. 2020. Food and Liquid Sensing in Practical Environments using RFIDs. In *17th USENIX Symposium on Networked Systems Design and Implementation* (NSDI 20). USENIX Association, Santa Clara, CA, 1083–1100. <https://www.usenix.org/conference/nsdi20/presentation/ha>
- [52] Chris Harrison and Scott E Hudson. 2008. Scratch input: creating large, inexpensive, unpowered and mobile finger input surfaces. In *Proceedings of the 21st annual ACM symposium on User interface software and technology*. 205–208.
- [53] Xuanke He, Jiang Zhu, Wenjing Su, and Manos M. Tentzeris. 2020. RFID Based Non-Contact Human Activity Detection Exploiting Cross Polarization. *IEEE Access* 8 (2020), 46585–46595. <https://doi.org/10.1109/ACCESS.2020.2979080>
- [54] Hamdan Hejazi, Husam Rajab, Tibor Cinkler, and László Lengyel. 2018. Survey of platforms for massive IoT. In *2018 IEEE International Conference on Future IoT Technologies (Future IoT)*. 1–8. <https://doi.org/10.1109/FIOT.2018.8325598>
- [55] Meng-Ju Hsieh, Jr-Ling Guo, Chin-Yuan Lu, Han-Wei Hsieh, Rong-Hao Liang, and Bing-Yu Chen. 2019. RFTouchPads: Batteryless and Wireless Modular Touch Sensor Pads Based on RFID. In *Proceedings of the 32nd Annual ACM Symposium on User Interface Software and Technology* (New Orleans, LA, USA) (UIST '19). Association for Computing Machinery, New York, NY, USA, 999–1011. <https://doi.org/10.1145/3332165.3347910>
- [56] Chen-Yu Hsu, Rumen Hristov, Guang-He Lee, Mingmin Zhao, and Dina Katabi. 2019. Enabling Identification and Behavioral Sensing in Homes Using Radio Reflections. In *Proceedings of the 2019 CHI Conference on Human Factors in Computing Systems* (Glasgow, Scotland Uk) (CHI '19). Association for Computing Machinery, New York, NY, USA, 1–13. <https://doi.org/10.1145/3290605.3300778>
- [57] Yasha Irvantchi, Yi Zhao, Kenrick Kin, and Alanson P. Sample. 2023. SAWSense: Using Surface Acoustic Waves for Surface-Bound Event Recognition. In *Proceedings of the 2023 CHI Conference on Human Factors in Computing Systems* (Hamburg, Germany) (CHI '23). Association for Computing Machinery, New York, NY, USA, Article 422, 18 pages. <https://doi.org/10.1145/3544548>

- 3580991
- [58] Haojian Jin, Jingxian Wang, Zhijian Yang, Swarun Kumar, and Jason Hong. 2018. WiSh: Towards a Wireless Shape-Aware World Using Passive RFIDs. In *Proceedings of the 16th Annual International Conference on Mobile Systems, Applications, and Services (Munich, Germany) (MobiSys '18)*. Association for Computing Machinery, New York, NY, USA, 428–441. <https://doi.org/10.1145/3210240.3210328>
- [59] Nacer Khalil, Mohamed Riduan Abid, Driss Benhaddou, and Michael Gerndt. 2014. Wireless sensors networks for Internet of Things. In *2014 IEEE Ninth International Conference on Intelligent Sensors, Sensor Networks and Information Processing (ISSNIP)*, 1–6. <https://doi.org/10.1109/ISSNIP.2014.6827681>
- [60] Atsutake Kosuge, Satoshi Suehiro, Mototsugu Hamada, and Tadahiro Kuroda. 2022. mmWave-YOLO: A mmWave Imaging Radar-Based Real-Time Multi-class Object Recognition System for ADAS Applications. *IEEE Transactions on Instrumentation and Measurement* 71 (2022), 1–10. <https://doi.org/10.1109/TIM.2022.3176014>
- [61] Gierad Laput and Chris Harrison. 2019. SurfaceSight: A New Spin on Touch, User, and Object Sensing for IoT Experiences. In *Proceedings of the 2019 CHI Conference on Human Factors in Computing Systems (Glasgow, Scotland UK) (CHI '19)*. Association for Computing Machinery, New York, NY, USA, 1–12. <https://doi.org/10.1145/3290605.3300559>
- [62] Gierad Laput, Yang Zhang, and Chris Harrison. 2017. Synthetic Sensors: Towards General-Purpose Sensing. In *Proceedings of the 2017 CHI Conference on Human Factors in Computing Systems (Denver, Colorado, USA) (CHI '17)*. Association for Computing Machinery, New York, NY, USA, 3986–3999. <https://doi.org/10.1145/3025453.3025773>
- [63] Chenning Li, Zheng Liu, Yuguang Yao, Zhichao Cao, Mi Zhang, and Yunhao Liu. 2020. Wi-Fi See It All: Generative Adversarial Network-Augmented Versatile Wi-Fi Imaging. In *Proceedings of the 18th Conference on Embedded Networked Sensor Systems (Virtual Event, Japan) (SenSys '20)*. Association for Computing Machinery, New York, NY, USA, 436–448. <https://doi.org/10.1145/3384419.3430725>
- [64] Tianhong Li, Lijie Fan, Mingmin Zhao, Yingcheng Liu, and Dina Katabi. 2019. Making the invisible visible: Action recognition through walls and occlusions. In *Proceedings of the IEEE International Conference on Computer Vision*. 872–881.
- [65] Tianxing Li, Qiang Liu, and Xia Zhou. 2016. Practical Human Sensing in the Light. In *Proceedings of the 14th Annual International Conference on Mobile Systems, Applications, and Services (Singapore, Singapore) (MobiSys '16)*. Association for Computing Machinery, New York, NY, USA, 71–84. <https://doi.org/10.1145/2906388.2906401>
- [66] Wei Li, Hewu Li, and Yong Jiang. 2014. A practical RF-based indoor localization system combined with the embedded sensors in smart phone. In *2014 International Wireless Communications and Mobile Computing Conference (IWCMC)*. 1177–1182. <https://doi.org/10.1109/IWCMC.2014.6906522>
- [67] Rong-Hao Liang and Zengrong Guo. 2021. NFCSense: Data-Defined Rich-ID Motion Sensing for Fluent Tangible Interaction Using a Commodity NFC Reader. In *Proceedings of the 2021 CHI Conference on Human Factors in Computing Systems (Yokohama, Japan) (CHI '21)*. Association for Computing Machinery, New York, NY, USA, Article 505, 14 pages. <https://doi.org/10.1145/3411764.3445214>
- [68] Jiao Liu, Guanlong Teng, and Feng Hong. 2020. Human Activity Sensing with Wireless Signals: A Survey. *Sensors* 20, 4 (2020). <https://doi.org/10.3390/s20041210>
- [69] Yi Liu, Weiqing Huang, Shang Jiang, Bobai Zhao, Shuai Wang, Siye Wang, and Yanfang Zhang. 2023. TransTM: A device-free method based on time-streaming multiscale transformer for human activity recognition. *Defence Technology* (2023). <https://doi.org/10.1016/j.dt.2023.02.021>
- [70] Sven Mayer, Xiangyu Xu, and Chris Harrison. 2021. Super-Resolution Capacitive Touchscreens. In *Proceedings of the 2021 CHI Conference on Human Factors in Computing Systems (Yokohama, Japan) (CHI '21)*. Association for Computing Machinery, New York, NY, USA, Article 12, 10 pages. <https://doi.org/10.1145/3411764.3445703>
- [71] C.D. Nugent, S.I. McClean, I. Cleland, and W. Burns. 2014. 13.18 - Sensor Technology for a Safe and Smart Living Environment for the Aged and Infirm at Home. In *Comprehensive Materials Processing*, Saleem Hashmi, Gilmar Ferreira Batalha, Chester J. Van Tyne, and Bekir Yilbas (Eds.). Elsevier, Oxford, 459–472. <https://doi.org/10.1016/B978-0-08-096532-1.01319-4>
- [72] Simon Olberding, Nan-Wei Gong, John Tiab, Joseph A Paradiso, and Jürgen Steimle. 2013. A cuttable multi-touch sensor. In *Proceedings of the 26th annual ACM symposium on User interface software and technology*. 245–254.
- [73] Maggie Orth, J. R. Smith, E. R. Post, J. A. Strickon, and E. B. Cooper. 1998. Musical Jacket. In *ACM SIGGRAPH '98 Electronic Art and Animation Catalog* (Orlando, Florida, USA) (SIGGRAPH '98). Association for Computing Machinery, New York, NY, USA, 38. <https://doi.org/10.1145/281388.281456>
- [74] Asil Oztekin, Foad M. Pajouh, Dursun Delen, and Leva K. Swim. 2010. An RFID Network Design Methodology for Asset Tracking in Healthcare. *Decis. Support Syst.* 49, 1 (apr 2010), 100–109. <https://doi.org/10.1016/j.dss.2010.01.007>
- [75] Patrick Parzer, Florian Perteneder, Kathrin Probst, Christian Rendl, Joanne Leong, Sarah Schuetz, Anita Vogl, Reinhard Schwoedlauer, Martin Kaltenbrunner, Siegfried Bauer, et al. 2018. Resi: A highly flexible, pressure-sensitive, imperceptible textile interface based on resistive yarns. In *Proceedings of the 31st Annual ACM Symposium on User Interface Software and Technology*. 745–756.
- [76] Ivan Poupayev, Nan-Wei Gong, Shihoko Fukuhara, Mustafa Emre Karagozler, Carsten Schwesig, and Karen E. Robinson. 2016. Project Jacquard: Interactive Digital Textiles at Scale. In *Proceedings of the 2016 CHI Conference on Human Factors in Computing Systems (CHI '16)*. Association for Computing Machinery, New York, NY, USA, 4216–4227. <https://doi.org/10.1145/2858036.2858176>
- [77] Swadhin Pradhan, Eugene Chai, Karthikeyan Sundaresan, Lili Qiu, Mohammad A. Khojastepour, and Sampath Rangarajan. 2017. RIO: A Pervasive RFID-Based Touch Gesture Interface. In *Proceedings of the 23rd Annual International Conference on Mobile Computing and Networking (Snowbird, Utah, USA) (MobiCom '17)*. Association for Computing Machinery, New York, NY, USA, 261–274. <https://doi.org/10.1145/3117811.3117818>
- [78] Aanjan Ranganathan, Boris Danev, and Srdjan Capkun. 2015. Proximity Verification for Contactless Access Control and Authentication Systems. In *Proceedings of the 31st Annual Computer Security Applications Conference (Los Angeles, CA, USA) (ACSAC '15)*. Association for Computing Machinery, New York, NY, USA, 271–280. <https://doi.org/10.1145/2818000.2818004>
- [79] Ammar Rayes and Samer Salam. 2022. *The Things in IoT: Sensors and Actuators*. Springer International Publishing, Cham, 63–82. [https://doi.org/10.1007/978-3-030-90158-5\\_3](https://doi.org/10.1007/978-3-030-90158-5_3)
- [80] Yili Ren, Sheng Tan, Linghan Zhang, Zi Wang, Zhi Wang, and Jie Yang. 2020. Liquid Level Sensing Using Commodity WiFi in a Smart Home Environment. *Proc. ACM Interact. Mob. Wearable Ubiquitous Technol.* 4, 1, Article 24 (mar 2020), 30 pages. <https://doi.org/10.1145/3380996>
- [81] Sanjay Sarma. 2004. Integrating RFID: Data Management and Inventory Control Are about to Get a Whole Lot More Interesting. *Queue* 2, 7 (oct 2004), 50–57. <https://doi.org/10.1145/1035594.1035620>
- [82] Syed Aziz Shah, Hasan Abbas, Muhammad Ali Imran, and Qammer H. Abbasi. 2021. RF Sensing for Healthcare Applications. *John Wiley Sons, Ltd, Chapter 8*, 157–177. <https://doi.org/10.1002/9781119695721.ch8> arXiv:<https://onlinelibrary.wiley.com/doi/pdf/10.1002/9781119695721.ch8>
- [83] Zhihui Shao, Mohammad A. Islam, and Shaolei Ren. 2020. Your Noise, My Signal: Exploiting Switching Noise for Stealthy Data Exfiltration from Desktop Computers. *Proc. ACM Meas. Anal. Comput. Syst.* 4, 1, Article 07 (may 2020), 39 pages. <https://doi.org/10.1145/3379473>
- [84] Joshua R. Smith, Kenneth P. Fishkin, Bing Jiang, Alexander Mamishev, Matthai Philipose, Adam D. Rea, Sumit Roy, and Kishore Sundara-Rajan. 2005. RFID-Based Techniques for Human-Activity Detection. *Commun. ACM* 48, 9 (sep 2005), 39–44. <https://doi.org/10.1145/1081992.1082018>
- [85] Ruiyuan Song, Dongheng Zhang, Zhi Wu, Cong Yu, Chunyang Xie, Shuai Yang, Yang Hu, and Yan Chen. 2022. RF-URL: Unsupervised Representation Learning for RF Sensing. In *Proceedings of the 28th Annual International Conference on Mobile Computing and Networking (Sydney, NSW, Australia) (MobiCom '22)*. Association for Computing Machinery, New York, NY, USA, 282–295. <https://doi.org/10.1145/3495243.3560529>
- [86] Sheng Tan, Yili Ren, Jie Yang, and Yingying Chen. 2022. Commodity WiFi Sensing in Ten Years: Status, Challenges, and Opportunities. *IEEE Internet of Things Journal* 9, 18 (2022), 17832–17843. <https://doi.org/10.1109/JIOT.2022.3164569>
- [87] Nicolas Villar, Daniel Cletheroe, Greg Saul, Christian Holz, Oscar Salandin, Tim Regan, Misha Sra, Hui-Shyong Yeo, William Field, and Haiyan Zhang. 2018. Project Zanzibar: A Portable and Flexible Tangible Interaction Platform. In *2018 ACM Conference on Human Factors in Computing Systems (CHI) (2018 acm conference on human factors in computing systems (chi) ed.)*. ACM. <https://www.microsoft.com/en-us/research/publication/project-zanzibar-portable-flexible-tangible-interaction-platform/> Best paper award.
- [88] Chen Wang, Jian Liu, Yingying Chen, Hongbo Liu, and Yan Wang. 2018. Towards In-baggage Suspicious Object Detection Using Commodity WiFi. In *2018 IEEE Conference on Communications and Network Security (CNS)*. 1–9. <https://doi.org/10.1109/CNS.2018.8433142>
- [89] Ge Wang, Shouqian Shi, Minmei Wang, Chen Qian, Cong Zhao, Han Ding, Wei Xi, and Jizhong Zhao. 2023. RF-Chain: Decentralized, Credible, and Counterfeit-Proof Supply Chain Management with Commodity RFIDs. *Proc. ACM Interact. Mob. Wearable Ubiquitous Technol.* 6, 4, Article 184 (jan 2023), 28 pages. <https://doi.org/10.1145/3569493>
- [90] Jingxian Wang, Chengfeng Pan, Haojian Jin, Vaibhav Singh, Yash Jain, Jason I. Hong, Carmel Majidi, and Swarun Kumar. 2020. RFID Tattoo: A Wireless Platform for Speech Recognition. *Proc. ACM Interact. Mob. Wearable Ubiquitous Technol.* 3, 4, Article 155 (sep 2020), 24 pages. <https://doi.org/10.1145/3369812>
- [91] Ju Wang, Jie Xiong, Xiaojiang Chen, Hongbo Jiang, Rajesh Krishna Balan, and Dingyi Fang. 2017. TagScan: Simultaneous Target Imaging and Material Identification with Commodity RFID Devices. In *Proceedings of the 23rd Annual*

- International Conference on Mobile Computing and Networking (Snowbird, Utah, USA) (MobiCom '17). Association for Computing Machinery, New York, NY, USA, 288–300. <https://doi.org/10.1145/3117811.3117830>
- [92] Saiwen Wang, Jie Song, Jaime Lien, Ivan Poupyrev, and Otmar Hilliges. 2016. Interacting with Soli: Exploring Fine-Grained Dynamic Gesture Recognition in the Radio-Frequency Spectrum. In Proceedings of the 29th Annual Symposium on User Interface Software and Technology (UIST '16). Association for Computing Machinery, New York, NY, USA, 851–860. <https://doi.org/10.1145/2984511.2984565>
- [93] Yichao Wang, Yili Ren, Yingying Chen, and Jie Yang. 2023. Wi-Mesh: A WiFi Vision-Based Approach for 3D Human Mesh Construction. In Proceedings of the 20th ACM Conference on Embedded Networked Sensor Systems (Boston, Massachusetts) (SenSys '22). Association for Computing Machinery, New York, NY, USA, 362–376. <https://doi.org/10.1145/3560905.3568536>
- [94] Zhong Lin Wang. 2013. Triboelectric Nanogenerators as New Energy Technology for Self-Powered Systems and as Active Mechanical and Chemical Sensors. *ACS Nano* 7, 11 (Nov. 2013), 9533–9557. <https://doi.org/10.1021/nn404614z> Publisher: American Chemical Society.
- [95] Zhong Lin Wang. 2014. Triboelectric nanogenerators as new energy technology and self-powered sensors – Principles, problems and perspectives. *Faraday Discuss.* 176 (2014), 447–458. Issue 0. <https://doi.org/10.1039/C4FD00159A>
- [96] Te-Yen Wu, Shutong Qi, Junchi Chen, Mujie Shang, Jun Gong, Teddy Seyed, and Xing-Dong Yang. 2020. Fabriccio: Touchless Gestural Input on Interactive Fabrics. In Proceedings of the 2020 CHI Conference on Human Factors in Computing Systems (Honolulu, HI, USA) (CHI '20). Association for Computing Machinery, New York, NY, USA, 1–14. <https://doi.org/10.1145/3313831.3376681>
- [97] Te-Yen Wu, Lu Tan, Yuji Zhang, Teddy Seyed, and Xing-Dong Yang. 2020. Capacitivo: Contact-Based Object Recognition on Interactive Fabrics using Capacitive Sensing. In Proceedings of the 33rd Annual ACM Symposium on User Interface Software and Technology (UIST '20). Association for Computing Machinery, New York, NY, USA. <https://doi.org/doi.org/10.1145/3379337.3415829> event-place: Virtual Event.
- [98] Te-Yen Wu and Xing-Dong Yang. 2022. iWood: Makeable Vibration Sensor for Interactive Plywood. In Proceedings of the 35th Annual ACM Symposium on User Interface Software and Technology, 1–12.
- [99] Robert Xiao, Greg Lew, James Marsanico, Divya Hariharan, Scott Hudson, and Chris Harrison. 2014. Toffee: enabling ad hoc, around-device interaction with acoustic time-of-arrival correlation. In Proceedings of the 16th international conference on Human-computer interaction with mobile devices & services, 67–76.
- [100] Chunyang Xie, Dongheng Zhang, Zhi Wu, Cong Yu, Yang Hu, and Yan Chen. 2023. RPM 2.0: RF-based Pose Machines for Multi-Person 3D Pose Estimation. *IEEE Transactions on Circuits and Systems for Video Technology* (2023), 1–1. <https://doi.org/10.1109/TCSVT.2023.3287329>
- [101] Hui-Shyong Yeo, Gergely Flamich, Patrick Schrempf, David Harris-Birtill, and Aaron Quigley. 2016. RadarCat: Radar Categorization for Input & Interaction. In Proceedings of the 29th Annual Symposium on User Interface Software and Technology (Tokyo, Japan) (UIST '16). Association for Computing Machinery, New York, NY, USA, 833–841. <https://doi.org/10.1145/2984511.2984515>
- [102] Chao Zhang. 2021. Intelligent Internet of things service based on artificial intelligence technology. In 2021 IEEE 2nd International Conference on Big Data, Artificial Intelligence and Internet of Things Engineering (ICBAIE), 731–734. <https://doi.org/10.1109/ICBAIE52039.2021.9390061>
- [103] Dingtian Zhang, Canek Fuentes-Hernandez, Raaghesh Vijayan, Yang Zhang, Yunzhi Li, Jung Wook Park, Yiyang Wang, Yuhui Zhao, Nivedita Arora, Ali Mirzazadeh, Youngwook Do, Tingyu Cheng, Saiganesh Swaminathan, Thad Starner, Trisha L. Andrew, and Gregory D. Abowd. 2022. Flexible computational photodetectors for self-powered activity sensing. *npj Flexible Electronics* 6, 1 (Jan. 2022), 7. <https://doi.org/10.1038/s41528-022-00137-z>
- [104] Diana Zhang, Jingxian Wang, Junsu Jang, Junbo Zhang, and Swarun Kumar. 2019. On the Feasibility of Wi-Fi Based Material Sensing. In The 25th Annual International Conference on Mobile Computing and Networking (Los Cabos, Mexico) (MobiCom '19). Association for Computing Machinery, New York, NY, USA, Article 41, 16 pages. <https://doi.org/10.1145/3300061.3345442>
- [105] Yang Zhang, Yasha Irvantchi, Haojian Jin, Swarun Kumar, and Chris Harrison. 2019. Sozu: Self-Powered Radio Tags for Building-Scale Activity Sensing. In Proceedings of the 32nd Annual ACM Symposium on User Interface Software and Technology (New Orleans, LA, USA) (UIST '19). Association for Computing Machinery, New York, NY, USA, 973–985. <https://doi.org/10.1145/3332165.3347952>
- [106] Yang Zhang, Gierad Laput, and Chris Harrison. 2018. Vibrosight: Long-Range Vibrometry for Smart Environment Sensing. In Proceedings of the 31st Annual ACM Symposium on User Interface Software and Technology (Berlin, Germany) (UIST '18). Association for Computing Machinery, New York, NY, USA, 225–236. <https://doi.org/10.1145/3242587.3242608>
- [107] Yang Zhang, Chouchang (Jack) Yang, Scott E. Hudson, Chris Harrison, and Alan-Son Sample. 2018. Wall++: Room-Scale Interactive and Context-Aware Sensing. In Proceedings of the 2018 CHI Conference on Human Factors in Computing Systems (Montreal QC, Canada) (CHI '18). Association for Computing Machinery, New York, NY, USA, 1–15. <https://doi.org/10.1145/3173574.3173847>
- [108] Cui Zhao, Zhenjiang Li, Han Ding, Ge Wang, Wei Xi, and Jizhong Zhao. 2022. RF-Wise: Pushing the Limit of RFID-based Sensing. In IEEE INFOCOM 2022 – IEEE Conference on Computer Communications, 1779–1788. <https://doi.org/10.1109/INFOCOM48880.2022.9796909>
- [109] Xuanjiao Zhu, Marcus Handte, and Rasit Eskicioglu. 2018. RF Technologies for Indoor Localization and Positioning. In Proceedings of the 16th ACM Conference on Embedded Networked Sensor Systems (Shenzhen, China) (SenSys '18). Association for Computing Machinery, New York, NY, USA, 428–429. <https://doi.org/10.1145/3274783.3275217>
- [110] Naor Zohar. 2022. Divide and Conquer: Detecting and Tracking Passive RFID Tags in Retail Spaces. In 2022 IEEE Wireless Communications and Networking Conference (WCNC) (Austin, TX, USA). IEEE Press, 1443–1448. <https://doi.org/10.1109/WCNC51071.2022.9771839>